Journal of Hydrology 625 (2023) 129982

Contents lists available at ScienceDirect

Journal of Hydrology

journal homepage: www.elsevier.com/locate/jhydrol

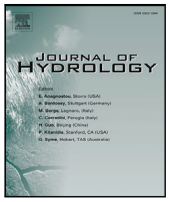

Research papers

HydroPol2D — Distributed hydrodynamic and water quality model: Challenges and opportunities in poorly-gauged catchments

Marcus Nóbrega Gomes Jr. [a,b,*], César Ambrogi Ferreira do Lago [a], Luis Miguel Castillo Rápalo [a], Paulo Tarso S. Oliveira [c], Marcio Hofheinz Giacomoni [b], Eduardo Mario Mendiondo [a,d]

[a] University of São Paulo, Department of Hydraulic Engineering and Sanitation, São Carlos School of Engineering, Av. Trab. São Carlense, 400 - Centro, São Carlos, 13566-590, São Paulo, Brazil

[b] The University of Texas at San Antonio, College of Engineering and Integrated Design, School of Civil Environmental Engineering and Construction Management, One UTSA Circle, BSE 1.310, San Antonio, 78249, TX, United States of America

[c] Faculty of Engineering, Architecture and Urbanism and Geography, Federal University of Mato Grosso do Sul, Brazil, Campo Grande, 79070–900, MS, Brazil

[d] I-SITE Excellence Program, University of Montpellier, Montpellier, France

ARTICLE INFO

This manuscript was handled by Nandita Basu, Editor-in-Chief, with the assistance of Andrea E. Brookfield, Associate Editor.

Dataset link: https://github.com/marcusnobrega-eng/HydroPol2D

Keywords:
2D hydrodynamic model
Water quality model
Build-up and wash-off
Water Adaptive Design
Low impact development
Pollutant transport and fate

ABSTRACT

Floods are one of the deadliest natural hazards and are exacerbated by changes in land-use and climate. Urban development decreases infiltration by reducing pervious areas and increases the accumulation of pollutants during dry weather. It also decreases infiltration by reducing pervious areas and increases the accumulation of pollutants during dry periods. During rainy events, there is an increase in pollution concentrations and runoff that may be a source of water supply during drought periods. Modeling the quantity and quality dynamics of stormwater runoff requires a coupled hydrodynamic module capable of estimating the transport and fate of pollutants. In this paper, we evaluate the applicability of a distributed hydrodynamic model coupled with a water quality model (HydroPol2D). First, the model is compared to GSSHA and WCA2D in the V-Tilted catchment, and the limitation of the critical velocity of WCA2D is investigated. We also applied the model in a laboratory wooden board catchment, focusing on the validation of the numerical approach to simulate water quality dynamics. Then, we apply HydroPol2D in the Tijuco Preto catchment, in São Carlos - Brazil, and compare the modeled results with the full momentum solver of the HEC-RAS 2D. This catchment shares similar characteristics with many poorly-gauged and human-impacted catchments worldwide. The implementation of the model, the governing equations, and the estimation of input data are discussed, indicating the challenges and opportunities to scale HydroPol2D into the reality of data scarcity of larger poorly-gauged catchments. For a 1-yr return period of rainfall and antecedent dry days, and assuming an uncertainty of 40% in the water quality parameters, the results indicate that the maximum concentration of total suspended solids (TSS), the maximum load and the mass of the pollutant washed in 30% of the volume are, 456 ± 260 $mgL^{-1}km^{-2}$, 2.56±0.4 $kgs^{-1}km^{-2}$, and 89% ± 10%, respectively.

1. Introduction

The spatial scale is a determinant factor to decide which tools to apply in water resources problems such as flood management (Kreibich et al., 2022), flood modeling (Gomes Jr et al., 2023), and spatial analysis of pollutants transport (Yanxia et al., 2022). Solutions to these problems typically require numerical modeling, and the quality of these models usually depends on data availability and the actual state-of-the-art conceptual models used to express complex phenomena of the water cycle.

Hydrologic, hydrodynamic, and pollutant transport models are fundamental tools for decision-making about mitigating floods and poor water quality (Fan and Collischonn, 2014). In the literature, there are a variety of models that aid in the quantification of hydrodynamic processes at different temporal and spatial scales. At the watershed scale, where these phenomena are usually expressed on larger time scales (e.g., hourly or daily), the Large-Scale Hydrological Model (MGB-IPH) (Collischonn et al., 2007; De Paiva et al., 2013) and the

* Corresponding author at: University of São Paulo, Department of Hydraulic Engineering and Sanitation, São Carlos School of Engineering, Av. Trab. São Carlense, 400 - Centro, São Carlos, 13566-590, São Paulo, Brazil.

E-mail addresses: marcusnobrega.engcivil@gmail.com (M.N. Gomes Jr.), cesar.dolago@utsa.edu (C.A.F. do Lago), luis.castillo@unah.hn (L.M.C. Rápalo), paulo.t.oliveira@ufms.br (P.T.S. Oliveira), marcio.giacomoni@utsa.edu (M.H. Giacomoni), emm@sc.usp.br (E.M. Mendiondo).

URL: http://www.engenheiroplanilheiro.com.br (M.N. Gomes Jr.).

https://doi.org/10.1016/j.jhydrol.2023.129982
Received 28 September 2022; Received in revised form 10 July 2023; Accepted 17 July 2023
Available online 25 July 2023

Hydrological Modeling and Analysis Platform (HyMAP) (Getirana et al., 2012) are examples.

At the scale of rapid response events and urban catchments, the Weighted Cellular Automata 2D (WCA2D) model (Guidolin et al., 2016), which uses the cellular automata approach to distribute runoff and estimate water surface flood maps, is another available model. Other fast flood models are available in the literature and focus mainly on simplifying non-linear hydrodynamic equations through assumptions such as the use of logic and linear runoff distribution rules (Jamali et al., 2018) or by data-driven approaches such as training neural networks to predict flood inundation maps (Kabir et al., 2020; do Lago et al., 2023).

Process-based models are typically more laborious than rapid flood models; however, they can better model events on the urban or rural scale and are not limited to the study area where they are applied. GSSHA (Gridded Surface/Subsurface Hydrologic Analysis) (Downer and Ogden, 2004) and SWAT (Soil and Water Assessment Tool) (Arnold et al., 2012), are examples of process-based models. GSSHA is often used to estimate hydrological-hydrodynamic processes and is also able to model sediment transport and fate (Furl et al., 2018; Sharif et al., 2017). However, few studies have used it for water quality assessment (Downer et al., 2015). Their approach to simulate soil detachment, sediment routing, and fines deposition is based on advection–dispersion equations, complete mixed reactors, and Shield's law. Similarly, other models such as the Water Quality Analysis Simulation Program (WASP) also use equations based on advection–dispersion to estimate the dynamics of sediment and water quality (Knightes et al., 2019).

Most of these methods require empirical parameters to represent hydraulic conditions, which can increase the complexity of the calibration due to the requirement of substantially more data, especially in poorly gauged catchments (Fu et al., 2019). Some recent examples of the application of 2D water quantity and quality models can be found in Shabani et al. (2021) and Yanxia et al. (2022). The research carried out in Shabani et al. (2021) coupled the Hydrologic Engineering Center - River System Analysis 2D (HEC-RAS 2D) with the Water Quality Analysis Simulation Program (WASP) and the results illustrate an approach of evaluation of the spatial distribution of soil detachment and Total Suspended Solids (TSS) during a flood event. Using a 2D diffusive-wave and advection-diffusion model, Yanxia et al. (2022) evaluated the concentrations of total phosphorus and total nitrogen. Both aforementioned investigations, however, were feasible to be validated due to extensive available field observations of discharges, concentrations, and pollutant loads.

In general, most studies on the dispersion and transport of pollutants address the pollution generated by agricultural sectors (Zia et al., 2013). For instance, the SWAT model has been used to predict and analyze the impacts of agricultural management practices at the watershed scale (Volk et al., 2016). Although able to model events on a sub-daily scale, only few articles worldwide used this model capability, and no articles with case studies in Brazil used it until 2019 (Brighenti et al., 2019).

The dynamics of pollutants in urban areas is complex and requires not only a complete description of physical, chemical, and biological phenomena at a proper spatial-temporal scale, but also a proper hydrological-hydrodynamic model that can explain the transport of pollutants in surface runoff (Vartziotis et al., 2022). These requirements are quite challenging in poorly gauged catchments. This could be the reason why many water quality analyzes are performed primarily with diluted metrics, such as event concentrations (EMC) or total maximum daily loads (TDML), rather than high-resolution pollutographs (Rossman and Huber, 2016).

For the sub-daily and sub-hourly temporal scales, a model capable of simulating water quality dynamics in a semi-distributed fashion is the Stormwater Management Model (SWMM). Although SWMM is typically applied for urban catchments, their conceptual model of semi-distributed modeling presents a limitation for the temporal-spatial distribution of pollutants in the catchment domain because modeled results are only visualized at nodes of links or at the outlet of sub-catchments. Simulating hydrodynamic and water quality processes and presenting results as maps with proper resolution is essential for understanding multiple issues. Spatial–temporal results can be used for problems such as (i) identifying prone areas to implement Low Impact Developments (LIDs) by estimating the potential pollutant retention, (ii) identifying areas prone to floods, and (iii) estimating pollutant concentrations in different locations in the domain. Therefore, to aid in the modeling of catchments with rapid hydrological response, HydroPol2D (Hydrodynamic and Pollution 2D Model) is developed. The model allows the distributed hydrodynamic modeling of surface runoff and the transport of pollutants in catchments and allows estimation of water quality and quantity dynamics at user-defined temporal and spatial resolutions.

HydroPol2D contributes to the field of hydrologic and hydrodynamic models by allowing a 2D flood and water quality modeling with the simulation of floodplain momentum transfer, spatially distributed infiltration and evapotranspiration calculation, and simulation of pollutant transport and fate. HydroPol2D also advances hydroinformatics by creating a fully explicit numerical model coupled with an adaptive time-stepping method to guarantee numerical stability for the water quantity and quality models of HydroPol2D. Moreover, HydroPol2D also allows the use of Graphics Processing Unit (GPU) calculations and have open source versions in Matlab and Python. This set of model capabilities is currently not available in the literature.

The main objective of the present work is to investigate the dynamics of surface runoff and water quality in a watershed with few available data - the Tijuco Preto catchment (TPC) in São Carlos/Brazil - and to highlight the potential of applying HydroPol2D in poorly gauged catchments. TSS as the overall water quality indicator (Di Modugno et al., 2015) and is modeled with HydroPol2D. In addition to simulating hydrodynamics and TSS transport in a poorly gauged catchment, we provide calibration and validation tests of HydroPol2D water quantity and quality components by applying the model in different case studies. To this end, the specific objectives of this paper are (i) to assess the velocity limitation of WCA2D by comparing HydroPol2D with GSSHA and WCA2D (Numerical Case Study 1), (ii) to calibrate and validate the water quality model of HydroPol2D (Numerical Case Study 2), and (iii) to compare HydroPol2D with HEC-RAS (Numerical Case Study 3), as well as to provide a comprehensive TSS spatial–temporal analysis.

2. Material and methods

2.1. HydroPol2D model

The main concept of the model is to simulate the transport of water and pollutant mass through the interaction between a central cell and its 4 neighbors (Von Neumann grid). HydroPol2D allows assessing the variation of surface runoff along the catchment in space and time based on their physical and morphological characteristics. The model consists of 3 major components: infiltration model (i.e., hydrologic model), non-linear reservoir + cellular automata approach (i.e., hydrodynamic model) and build-up and wash-off model (i.e., water quality model).

The main parameters of the model are presented in Table 1. In addition, the model requires georeferenced .TIFF rasters that represent topography (Digital Elevation Model), land use and cover (LULC), and soil type. From these maps, we derive distributed parameters for each component of the model. Hydrologic Model parameters are determined in terms of the soil raster (e.g., infiltration parameters of Green-Amp model (Green W. H, 1911)), whereas the parameters of the Hydrodynamic Model (e.g., Manning's coefficient (Chow, 2010)) are described by the LULC. Similarly, the Water Quality Model parameters (e.g., Build-up and Wash-off parameters (Rossman and Huber, 2016)) are also entered as a function of LULC. All model components can have

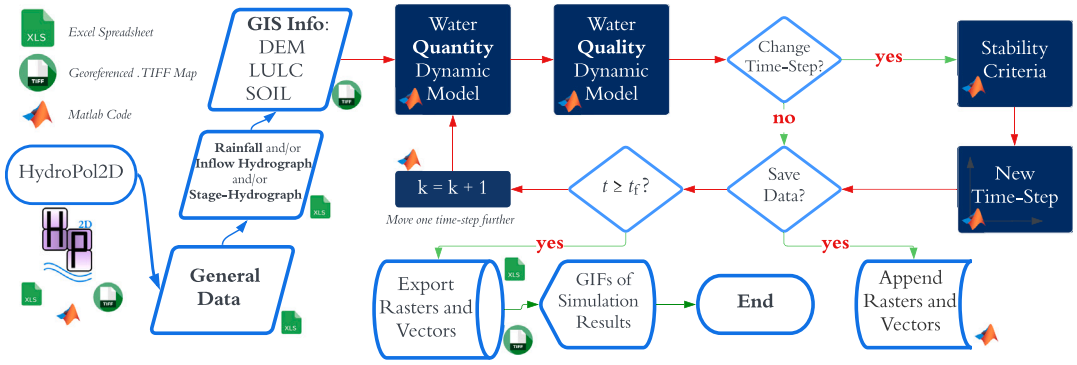

Fig. 1. HydroPol2D model flowchart, where t_f represents the final simulation time and k represents the current time-step number. The *General Data* input sets final processing parameters, stability, and all other numerical parameters, i.e., not in matrix or vector format; The *Rainfall and/or Inflow Hydrograph and/or Stage-Hydrograph* sets the input rain-on-the-grid boundary conditions and/or punctual inflows and stages at internal nodes of the model. In addition, it defines the cells that receive this input hydrograph. At least one internal boundary condition has to be set. Finally, the *GIS Info* input data defines the digital elevation model and the land use land cover map. map.

Table 1
Input data as a function of LULC and Soil Maps. HydroPol2D require the units for each variable as presented in this table. The model requires a minimum of 11 parameters to simulate the water quantity and quality dynamics.

Model	Variable	Symbol (units)	Source of uncertainty
Hydrologic Model	Saturated Hydraulic Conductivity	k_{sat} (mm h^{-1})	Spatial Variability
	Suction Head	ψ (mm)	Seasonality and Soil Loss
	Moisture Deficit	$\Delta\theta$ (cm^3 cm^{-3})	Inter-event Variability
	Initial Soil Moisture	I_0 (mm)	Inter-event Variability
Hydrodynamic Model	Manning's Roughness Coefficient	n (s m$^{-1/3}$)	Stage Variability
	Initial Abstraction	h_0 (mm)	Spatial Variability
	Initial Water Surface Depth	d_0 (mm)	Warm-up Process
Water Quality Model	Linear Build-up Coefficient	C_1 (kg ha^{-1})	Spatial Variability
	Exponential Build-up Coefficient	C_2 (day^{-1})	Temporal Variability
	Linear Wash-off Coefficient	C_3 (–)	Spatial Variability
	Exponential Wash-off Coefficient	C_4 (–)	Spatio-Temporal Variability

initial values entered according to each category of its input data, or can have input maps representing initial conditions. More details on how to obtain and estimate the parameters used in the model can be found in Gomes Jr. et al. (2021). The flowchart of the model steps is presented in Fig. 1.

First, HydroPol2D reads the input data and the boundary conditions of rain-on-grid, inflow hydrograph, and stage-hydrograph. The model requires at least one of the aforementioned boundary conditions to perform the numerical calculations. It also reads the downstream boundary condition that can be modeled either as normal flow or critical flow (Kollet and Maxwell, 2006). Then, HydroPol2D discretizes the time domain and calculates two main processes: it solves the water quantity dynamic system presented in Eq. (3), and the water quality dynamic system shown in Eq. (9). Following this process, it decides whether to change the time step or not following Eq. (19), append rasters and vectors of the main states (e.g., water depths, infiltrated depths, stored pollutant mass) and check if the simulation time (t_f) is reached. The numerical modeling is carried out until t_f = simulation time.

2.1.1. Water quantity model - 2D conservation of mass and momentum

The HydroPol2D model solves mass balance and momentum conservation equations using the diffusive wave approximation to estimate the outflow of each cell O (mm h^{-1}) in Eq. (1). However, the diffusive wave equation is only solved for the steepest water surface slope for each cell. Each cell can potentially have four flow directions and hence 4 water surface slopes gradients. Therefore, the model solves the non-linear Manning's equation (i.e., relatively computationally expensive due to power functions required) only once per cell. For the remainder of the directions, it solves the distribution of runoff through simplification using rules of cellular automata (Guidolin et al., 2016) based on the available void volume in the boundary cells. The primary input data for the hydrological module are the spatial and temporal distribution of rainfall intensity, inflow hydrographs, stage-hydrographs, as well as the identification of downstream boundary conditions. Cell topology and connections between them, follow the Cartesian directions in a 2D spatial mesh of Von Neumann with y–y and x–x flow directions.

Let D be the catchment domain containing all cells that represent the physical region of interest and let the superscript (i, j) represent the ith and jth cell $\in D$. Also, let $\mathcal{N}^{i,j}$ be the sub-domain represented by the four neighbors of the cell i, j. The following description of the model equations are dimensionally homogeneous with units in the international system, except when clearly stated different. Combining the main elements of the mass balance in a cell (i.e., a pixel with known resolution), we can describe the rate of change in water surface depth in cell i, j as (Rossman et al., 2010):

$$\frac{\partial d^{i,j}(t)}{\partial t} = \left[\sum_{\mathcal{N}^{i,j}} I^{i,j}(t) - \sum_{\mathcal{N}^{i,j}} O^{i,j}(t) + i^{i,j}(t) - f^{i,j}\left(d^{i,j}(t), F_d^{i,j}(t)\right) - e_T^{i,j}(t)\right] \quad (1)$$

where $d^{i,j}(t)$ is the water surface depth (m), $I^{i,j}(t)$ is the inflow rate (LT^{-1}), $O^{i,j}(t)$ is the outflow rate (LT^{-1}), $i^{i,j}(t)$ is the rainfall intensity (LT^{-1}), $f^{i,j}(t)$ is the infiltration rate (LT^{-1}), $F_d(t)$ is the infiltrated depth of water into the soil (L), and $e_T^{i,j}(t)$ is the evapotranspiration rate (LT^{-1}).

Infiltration of water into the soil is represented using the Green and Ampt (GA) model (Green W. H, 1911), which can be derived from a simplification of Richards equation (Richards, 1931), and is applied to each cell of the spatial mesh created for the discretization of the catchment. Infiltration capacity is modeled as:

$$C_f^{i,j}(t) = k_{sat}^{i,j}\left[1 + \frac{\left(\psi^{i,j} + d^{i,j}(t)\right)}{L^{i,j}(t)}\right] \quad (2)$$

where $C_f^{i,j}(t)$ is the infiltration capacity (LT^{-1}), $k_{sat}^{i,j}$ is the saturated hydraulic conductivity (LT^{-1}), $L(t) = \frac{F_d(t)}{\Delta\theta}$ is the wetting front depth (L), and $\psi^{i,j}$ is the suction head (L).

The infiltration rate is the minimum value between the infiltration capacity and the water availability rate and can be calculated for a time $t+\Delta t$ with inflow rates, depths, and infiltrated depths from t. Expanding Eq. (1) by a 1st order Taylor's approximation, we can derive a forward in time explicit numerical solution for the 2D water surface dynamics problem by neglecting the high order terms, such that:

$$d^{i,j}(t+\Delta t) = d^{i,j}(t) + \Delta t\left[\sum_{\mathcal{N}^{i,j}} I^{i,j}(t) - \sum_{\mathcal{N}^{i,j}} O^{i,j}(t) + i^{i,j}(t) - f^{i,j}\left(d^{i,j}(t), F_d^{i,j}(t)\right) - e_{\mathrm{T}}^{i,j}(t)\right] \quad (3)$$

The current version of the model allows for the simulation of soil moisture restitution during dry weather periods and the spatial simulation of evapotranspiration through Penman-Monteith simulation, which aids in the modeling of droughts (Melo et al., 2023). In addition, it allows modeling space-variant rainfall through interpolation methods such as the inverse-distance-weightning and allows to enter user-defined rainfall maps derived from radar or sattelite imagery. Although these characteristics are not directly investigated in this article, they are available in the model repository (Gomes Jr., 2023) and explained in the supplemental material. During wet weather periods, the state variable $L^{i,j}(t)$ (i.e., the saturated depth of the wetting front) is calculated only by integrating the infiltration rate over time (Gomes Jr. et al., 2021). Therefore, the initial value of $L^{i,j}(0)$ can be calibrated to represent the initial conditions of proper soil moisture and can be entered as an input map in the model that represents the initial conditions of soil moisture for each cell.

The conversion of depth to flow is done through the calculations of I and O of Eq. (1) based on the Manning's equation using the friction slope that is calculated from the water surface elevation steepest gradient. In this model, the friction slope is assumed to be equal to the slope of the energy line (i.e., diffusive wave (Vieira, 1983)). Therefore, to distribute the volumes of surface runoff to the boundary cells, a system of weighted averages is performed in terms of the void volumes available between neighboring cells, substantially reducing the calculations by calculating the runoff velocity only for the direction of the highest slope of the water surface (Guidolin et al., 2016) and distributing the surface runoff volume as a function of this weighted average.

It is important to note that although the Manning equation is typically used for steady-state and uniform flow, it does not necessarily occur in the HydroPol2D model because the slope of the energy line is not assumed as the bottom slope. Therefore, this modeling capability allows HydroPol2D to estimate hydraulic transients and to dynamically change flow direction according to water surface elevation slopes. Moreover, HydroPol2D can also simulate backwater effects and river networks with bifurcations due to its adaptive flow direction scheme according to water surface elevations. A detailed pseudo-code of the model internal processes to solve Eq. (3) with the Cellular-Automata approach is presented in the Supplemental Material.

2.1.2. Critical velocity limitation

Two versions of the HydroPol2D model were developed with respect to how flow velocities are treated, herein we name them as HydroPol2D (a) and HydroPol2D (b). For example, the research conducted in Guidolin et al. (2016) restricted flow velocities to the critical velocities in their WCA2D model - a similar modeling approach to HydroPol2D. However, several studies point out that hydrodynamic modeling, especially in significant flooding events, can present a mixed flow regime (i.e., the regime can change from sub-critical to super-critical flow rapidly) (Farooq et al., 2019). Therefore, some areas in the domain might have flow velocities larger than the critical velocity. The two adaptations of the HydroPol2D model (a) and (b) are available and are described below with respect to the critical velocity as follows:

- HydroPol2D (a): Change of hydraulic regime is allowed and the flow velocity is unconstrained; however, hydraulic jump is not modeled due to diffusive wave model that does not account for convective and local acceleration features presented in full dynamic wave models. This model assumption is more applicable for high-resolution flood inundation mapping and modeling.
- HydroPol2D (b): The flow velocity is constrained to the critical flow, ensuring only sub-critical or fluvial flow regime in all cells of the domain. In this case, there are relatively lower velocities and, as a consequence, longer time-steps and shorter simulation durations. Moreover, this limitation might affect flood wave propagation and hence delay peak times.

These two variations of the model can be controlled by a factor f_m and result from the limitation of the maximum flow velocity, given by Eqs. (4) and (5):

$$v_{\mathrm{m}}^{i,j}(t) = \min\left(f_{\mathrm{m}}\sqrt{g h_{ef}^{i,j}(t)}, \frac{1}{n^{i,j}}\Delta x\left(h_{ef}^{i,j}(t)\right)^{\frac{5}{3}}\sqrt{s_e^{i,j}(t)}\right) \quad (4)$$

$$h_{ef}^{i,j}(t) = \max\left(d^{i,j}(t) - h_0^{i,j}, 0\right) \quad (5)$$

where v_m is the maximum velocity calculated for the steepest direction (m s^{-1}), g gravity acceleration (m s^{-2}), d is the water surface depth (m), f_m is a factor assumed to account for models HydroPol2D (a) and HydroPol2D (b), s_e (m m^{-1}) is the steepest slope of the water surface calculated from the water surface elevation map, Δx is the spatial discretization of cells (m), n is the Manning's roughness coefficient (s $m^{-1/3}$), and h_{ef} is the effective water surface depth considering losses through the initial abstraction (m) (h_0), with h_0 in (m).

In the case of model HydroPol2D (a), f_m can be assumed to tend to infinity, such that it does not limit the flow to the critical velocity, otherwise $f_m = 1$. The previous formula is applied to each time-step, for all cells of the domain, but only to the direction of the steepest water surface slope.

2.1.3. Water quality modeling - 2D build-up and wash-off

The mathematical model used to determine the transport and fate of pollutants is based on the build-up and wash-off model (Deletic, 1998; Rossman and Huber, 2016). The term build-up refers to the accumulation of pollutants in the catchment during dry periods, and the term wash-off refers to the washing and transport of these pollutants during wet periods events (Rossman and Huber, 2016). Several mathematical formulations for this model are proposed and, in this article, an adaptation of the exponential build-up and wash-off model is assumed. Furthermore, the increase in pollutants (ΔB) in the catchment during dry weather periods is assumed as a variable dependent only on the number of consecutive dry days (ADD), as shown in Eq. (6):

$$\Delta B_l^{i,j} = 10^{-4} A_c\left[C_{1,l}^{i,j}\exp\left\{-C_{2,l}^{i,j}\mathrm{ADD}\right\}\right] \pm R_l(\mathrm{ADD}) \quad (6)$$

where C_1 is the build-up coefficient, function of land use and land cover (kg ha^{-1}), C_2 is the daily accumulation rate of build-up (day^{-1}), ADD is the antecedent dry days (days), A_c is the area of (m^2), l represents the classification of land use (e.g., pervious or impervious areas) and we introduce a source term R to allow modeling of a non-conservative mass balance due to self-degradation or chemical reaction, varying for each land use and land cover (kg ha^{-1}).

The Eq. (6) is valid in dry periods and calculates the build-up increment which, if added to the initial build-up, represents the amount of mass available in each cell at the end of the ADD time (Deletic, 1998). Typically, for total suspended solids, R can be neglected. The original equation of the exponential wash-off model, which acts on the equation of the build-up variation during the wet weather periods, can be modeled as follows in Eq. (7)

$$\frac{\mathrm{d}B(t)}{\mathrm{d}t} = -W_{out}(t) = 10^{-4} A_c\left(-C_3^* q(t)^{C_4^*} B(t)\right) \quad (7)$$

where C_3^* and C_4^* are wash-off coefficients in terms of specific flow rates (i.e., flow divided by catchment area) instead of flow discharges in each cell. The variable $q(t)$ is the flow rate usually given in (mm h^{-1}) or (in h^{-1}) and can be inferred by dividing the outlet flow by the catchment area when the catchment is modeled in a concentrated model (Xiao et al., 2017). The units of C_3^* depend on the units of $q(t)$, which is used in the conversion factor of C_4^* so that it guarantees that the wash-off rate W has units of mass/time or (e.g., kg h^{-1}). In summary, for the international system of units C_3 has dimensions of $(LT^{-1})^{C_4}T^{-1}$, depending on $q(t)$ (Rossman and Huber, 2016).

The Eq. (7) is used in the SWMM software and is applied in a concentrated hydrologic conceptual model, assuming a single representative value for the entire sub-catchment, as aforementioned. To represent the wash-off phenomenon, we have used a variation of the previously presented exponential model of wash-off (Shaw et al., 2006; Tu and Smith, 2018; Wicke et al., 2012; Wijesiri et al., 2015a). The adaptation made in HydroPol2D is the following: instead of modeling the wash-off using functions dependent on specific flow rates (equivalent depth per unit of time), the model calculates the transport of pollutants, that is, rate of pollution washed, as a function of the flow discharges leaving each cell and its available mass to be washed. Another significant difference is that pollutants enter and leave cells simultaneously wet weather periods. This feature changes the mass balance equation so that the equation for the rate of change of the mass of pollutants can be written as a combination of inputs and outputs of pollutant mass given by:

$$\frac{\partial B^{i,j}(t)}{\partial t} = \sum_{\forall\ \mathrm{dir}} W^{i,j}_{\mathrm{in,dir}}(t) - \sum_{\forall\ \mathrm{dir}} \overbrace{C_3\left(Q^{i,j}_{\mathrm{dir}}(t)\right)^{C_4} f\left(B(t)\right)}^{W^{i,j}_{\mathrm{out,dir}}(t)}, \tag{8}$$

where W is the wash-off load (kg h^{-1}), the sub-index *in* and *out* represent the inlet and outlet of the cells, respectively. The sub-index dir represents the flow direction, varying among leftwards, rightwards, upwards, and downwards, respectively, following the Cartesian directions. $W_{\mathrm{in,dir}}(t)$ is the rate of pollutant inflow in direction dir, and the term $\sum_{\forall\ \mathrm{dir}} W^{i,j}_{\mathrm{in,dir}}(t)$ calculates the pollutant inflow rate and depends on the topology of the problem. Q_{dir} is the outflow discharge ($m^3\ s^{-1}$) into direction dir, and $f(B(t))$ is explained further.

Discretizing Eq. (8) using a forward Euler scheme, it follows that:

$$B^{i,j}(t+\Delta t) = B^{i,j}(t) + \Delta t\overbrace{\left(\sum_{\forall\ \mathrm{dir}} W^{i,j}_{\mathrm{in,dir}} - \sum_{\forall\ \mathrm{dir}} W^{i,j}_{\mathrm{out,dir}}(t)\right)}^{\Delta W^{i,j}(t)} \tag{9}$$

The function $f(B(t))$ varies the equation of pollutant washing according to the mass accumulated in the cells. For values of $B(t)$ smaller than B_{min}, the pollutant flux is assumed to be zero. This is the typical case of pollutants that are fixed on the soil and surface and are difficult to wash-off. For values greater than B_{min} but smaller than a threshold B_{r}, which depends on the type of pollutant, the washing rate follows a sediment rating curve independent of the accumulated mass; therefore, washing is exclusively dependent on the rating curve coefficients, which are equal to the wash-off coefficients. Note that B_{r} can be assumed equals B_{min}, that is, the effect of the rating curve can be neglected. For the cases where the available mass is between B_{r} and B_{m}, where B_{m} is an upper bound, the wash rate is scaled (see Fig. 2) by the mass of pollutants in the cell, following the typical exponential wash-off model (Rossman et al., 2010). In the cases where $B(t)$ is greater than B_{m}, the maximum output rate is limited to the representative value of B_{m}. These conditions are expressed in Eq. (10), such that:

$$f\left(B(t)\right) = \begin{cases} 0, \ \text{if}\ B(t) \le B_{\mathrm{min}} \\ 1, \ \text{if}\ B_{\mathrm{min}} \le B(t) \le B_{\mathrm{r}} \\ \left(1 + B(t) - B_{\mathrm{r}}\right), \ \text{if}\ B_{\mathrm{r}} \le B(t) \ge B_{\mathrm{m}} \\ \left(1 + B_{\mathrm{m}} - B_{\mathrm{r}}\right), \ \text{if}\ B(t) \ge B_{\mathrm{m}}. \end{cases} \tag{10}$$

The imposition of a B_{min} value on the pollutant washing rate substantially improves the computational performance of the model by avoiding calculations in cells where the accumulated mass tends to zero and, therefore, avoids the minimum time-step tending to zero. Furthermore, the choice of the limit B_r is effective as it ensures that pollutants follow a rating curve model for relatively low accumulated masses but larger than a minimum value B_{r}. For instance, if the conventional wash-off model were used (Eq. (7)), the mathematical operation to calculate the wash-off rate $C_3\ Q^{C_2}B(t)$ would tend to zero if B(t) tends to zero. This might result in a non-realistic case, especially when considering a relatively low available pollutant mass washed by a large flow rate that would have nearly no wash-off because B(t) tends to zero.

Previous modeling results indicate that for TSS, $B_{\mathrm{min}} = 1\ g\ m^{-2}$, $B_{\mathrm{r}} = 10\ g\ m^{-2}$, and $B_{\mathrm{m}} = 100\ g\ m^{-2}$ is consistent with TSS modeling in urban areas. These values can also be calibrated for different pollutants. Other studies of build-up and wash-off modeling (Hossain et al., 2012; Wicke et al., 2012) have applied the exponential wash-off equation presented in Eq. (7) in the form of specific flow rates (i.e., outlet flow divided by the catchment area) instead of the flow discharges. However, in these studies, concentrated hydrological models of the watershed are used to represent the dynamics of surface runoff in the watershed. If we write the flow as a function of the specific flow rate (q), we can derive the relationship between the two modeling approaches and compare the coefficients adopted in the literature. Assuming that the specific flow rate is given in (mm h^{-1}) and the modeled flow is in ($m^3\ s^{-1}$), we can write Eq. (11) relating the specific flow rate to the cell outlet flow discharge, such that:

$$Q_d(t) = \left(\frac{1}{3600 \times 1000}\right) q(t)\, \Delta x^2 \tag{11}$$

Finally, analogously using Eqs. (7) and (8), we can relate the coefficients C_3^* and C_4^* (that is, the coefficients considering the catchment as concentrated) with C_3 and C_4 (i.e., coefficients for distributed modeling), resulting in:

$$C_3 = \overbrace{\left(\frac{3600 \times 1000}{\Delta x^2}\right)^{C_4^*}}^{f_c} C_3^*, \quad C_4 = C_4^* \tag{12}$$

where f_{c} converts $C_3{}^*$ developed for q(t) in (mm h^{-1}) to the model proposed here using flow discharges in ($m^3\ s^{-1}$). The usual values of f_{c} are presented in Fig. S1 for various values of C_4 and can be used for comparison between SWMM parameters and the parameters suggested in the HydroPol2D model.

Using the previous states modeled with the aforementioned equations, we calculate water quality dynamic indicators such as the instantaneous pollutant concentrations in Eq. (13) and pollutant loads in Eq. (14) as follows:

$$C^{i,j}_{\mathrm{dir}}(t) = \lim_{\Delta t \to 0}\left(\frac{W^{i,j}_{\mathrm{out,dir}}(t)\Delta t}{Q^{i,j}_{\mathrm{out,dir}}(t)\Delta t}\right) \tag{13}$$

$$L^{i,j}_{\mathrm{dir}}(t) = C^{i,j}_{\mathrm{dir}}(t) Q^{i,j}_{\mathrm{out,dir}}(t) \tag{14}$$

The HydroPol2D model also allows the calculation of event mean concentration (EMC) and the first-flush curve that combines the normalized pollutant washed mass (m/M) with the normalized runoff volume (v/V) (Di Modugno et al., 2015). Let t_f be the end of an event and ϕ represent the outlet cells, one can calculate these time-varying metrics as follows:

$$\mathrm{EMC}^{\phi}(t) = \frac{\int_0^t W^{\phi}_{out}(t)\mathrm{d}t}{\int_0^{t_f} Q^{\phi}_{\mathrm{out}}(t)\mathrm{d}t} \tag{15a}$$

$$\frac{m^{\phi}(t)}{M^{\phi}} = \frac{\int_0^t W^{\phi}_{\mathrm{out}}(t)\mathrm{d}t}{\int_0^{t_f} W^{\phi}_{\mathrm{out}}(t)\mathrm{d}t} \tag{15b}$$

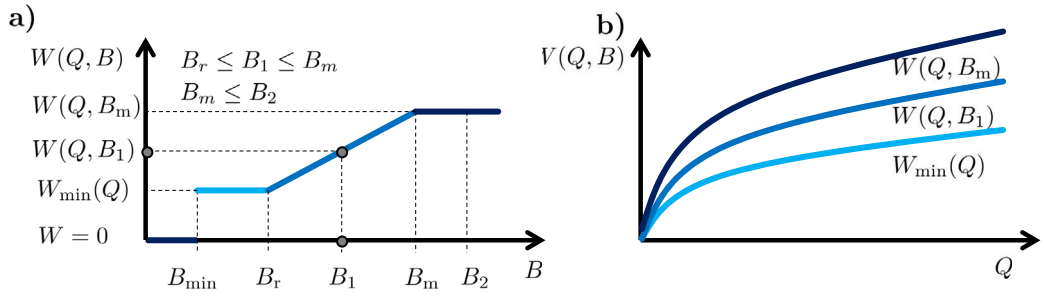

Fig. 2. Scheme of pollutant washing curves. Part (a) represents the washing rate as a function of accumulated mass for several cases, assuming a constant flow rate Q. Part (b) represents the pollutant rating curve as a function of the accumulated mass in terms of the flow discharge. This figure shows the envelope of rating curves assumed for the pollutant washing.

$$\frac{V^{\phi}(t)}{V^{\phi}} = \frac{\int_0^t Q_{\text{out}}^{\phi}(t)\mathrm{d}t}{\int_0^{t_f} Q_{\text{out}}^{\phi}(t)\mathrm{d}t} \tag{15c}$$

2.1.4. Numerical stability and adaptive time-stepping

For the numerical solution, either constant or adaptive time-steps can be used. The adaptive time-step values depend on the propagation conditions of the information along the cell computational mesh grid. In other words, to ensure that the information (i.e., wave propagation) does not exceed more than one cell in a time-step, the Courant–Friedrichs–Lewy (*CFL*) condition is considered as the numerical stability criterion, expressed in Eq. (16) as (Courant et al., 1928):

$$\Delta t^{r}(t) = \min_{\mathcal{D}}\left(\frac{\alpha^{r}\max_{\forall\ \text{dir}}\left(u_{\text{dir}}^{i,j}(t)\right)}{\Delta x}, \Delta t^{*}\right)\ \forall\ i,j\ \in \mathcal{D} \tag{16}$$

where α^{r} is a factor < 1 that ensures a courant number below the unit for the modeling of surface runoff, Δt* is the maximum time-step assumed in the simulation, the sub-index (dir) represents an orthogonal direction from cell $i,j \in \mathcal{D}$, and u is the wave celerity, given by Eq. (17):

$$u_{\text{dir}}^{i,j}(t) = \left|v_{\text{dir}}^{i,j}(t)\right| \pm \sqrt{g d^{i,j}(t)} \tag{17}$$

where v is the wave velocity.

Some degree of numerical diffusion occurs when using very low values of α^{r} and must be previously assessed to ensure more accurate numerical solutions (Lantz, 1971). For water quality, we must ensure that the available pollutant mass does not reach negative values in each time-step. This is the typical case when a long time-step is used. Fig. 3 presents a schematic of the pollutant transport model that illustrates the processes of numerical stability and mass balances. By dividing the available pollutant mass by the pollutant wash-off for all cells in the domain, the minimum time-step is obtained to ensure numerical stability, expressed in Eq. (18) as:

$$\Delta t^{q}(t) = \min_{\mathcal{D}}\left(3600\frac{\alpha^{q} B^{i,j}(t)}{|\Delta W^{i,j}(t)|}, \Delta t^{*}\right)\ \forall\ i,j \in \mathcal{D},\ \text{If}\ \Delta W^{i,j}(t) < 0 \tag{18}$$

where ΔW_{out} is the outflow flux of pollutants leaving the cell (i.e., the net wash-off) considering the 4 directions, that is, the difference between outflow and inflow of pollutant loads (kg h^{-1}), and Δt^* is the minimum time-step assumed in the model (s).

Theoretically, the model should not have a minimum time-step constraint Δt^* to be considered numerically stable. However, as shown in Eq. (18), the time-step tends to zero as $B(t)$ approaches zero. This implies that after the first-flush, which eventually washes most of the initial pollutants out of the catchment and causes $B(t)$ to tend to zero, the time-step would also tend to zero. Therefore, we assume the minimum water quality time-step (Δt^*). Finally, the chosen time-step of the model considers the stability of both water quality and quantity models as follows:

$$\Delta t(t) = \min\left[\Delta t^{r}(t), \Delta t^{q}(t)\right] \tag{19}$$

2.2. Numerical case study 1 — V-tilted catchment

The first case study is performed in a synthetic catchment (V-Tilted Catchment) that has been used to test surface runoff models (Fry and Maxwell, 2018; Gomes Jr. et al., 2022; Kollet and Maxwell, 2006) and we compare HydroPol2D in this catchment with GSSHA. The objective of this numerical case study is twofold: assess the influence of space and time discretization and investigate the limitation of critical velocity. This theoretical catchment has only one outlet pixel and is assumed to have a width equal to the spatial discretization resolution of the cell grid (20 m × 20 m). The V-Tilted catchment corresponds to a catchment of 1,620 m × 1,000 m (area = 1.62 km^2) composed of two rectangular planes (i.e., hillslopes) measuring 800 m × 1000 m, each coupled with a vegetated channel in the connection of the two planes (Gomes Jr. et al., 2022). The slope in the x–x direction is 5%, while the slope in the y–y direction is 2%, as shown in Fig. 4(a).

Two types of ground cover are assumed: channel (n = 0.15 s m$^{-1/3}$) and hillslopes (n = 0.015 s m$^{-1/3}$). Only surface runoff flow is evaluated; therefore, infiltration, water quality, and runoff generated by excess saturation are not modeled in this first test. A constant rainfall rate of 10.8 mm h^{-1} during 90 min is applied uniformly in the catchment. The gradient boundary condition (e.g., normal flow at the outlet) was assumed for a slope equal to the natural slope of the outlet channel. The calculation time is defined as 240 min to ensure the propagation of the hydrograph through the catchment. Fig. 4 (a) represents the digital terrain. Different time-step discretizations are tested, ranging from 0.1 to 60 s. In addition, an adaptive time-step numerical scheme is also evaluated, and simulated hydrographs with different computational meshes are compared.

2.3. Numerical case study 2 — wooden-plane catchment

This numerical case study aims to validate the proposed distributed water quality modeling. The water quality model, however, requires a calibrated water quantity model to predict discharges, and hence the pollutant rates. We applied the HydroPol2D model in a wooden board catchment of 3 m length and 1.5 m width that represents an impervious surface, as shown in Fig. 4(b) (Xiao et al., 2017; Zhang et al., 2020). The Manning's roughness coefficient (n) is spatially invariant and is assumed to be equal to 0.04 s m$^{-1/3}$, and the initial depth of the water is assumed to be 0.5 mm (Zhang et al., 2020). Rainfall is uniformly distributed in the catchment. All experimented events had a rainfall duration of 28 min. Previous modeling comparisons of HydroPol2D with flow observations in this catchment presented in Xiao et al. (2017) show good agreement. Therefore, the water quantity results were assumed as calibrated. In the study presented in Zhang et al. (2020), salt was used as the solute and all the experiments carried out were carried out evenly distributing 125 g of salt through the wooden board.

In this paper, we selected two cases of experiments presented in Zhang et al. (2020) with different conditions of rainfall and slope. Events 1 to 4 have slopes of 0.5° with rainfall intensities of 24.22, 43.16,

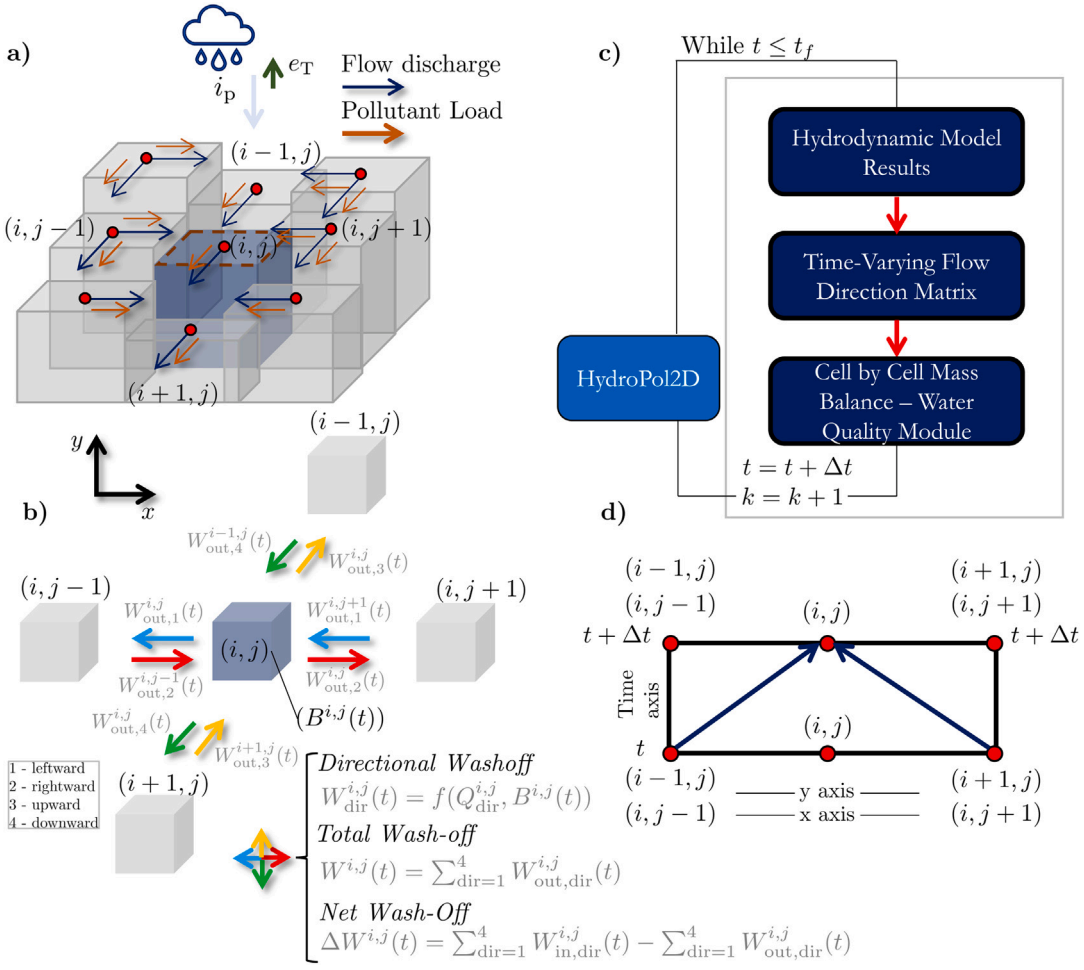

Fig. 3. Scheme of the pollutant transport model, where (a) represents a 3D schematic of a watershed with inflows and outflows and pollutants, (b) represents a cell with pollutant outflow rates W with pollutant outflow and inflow rates as a function of the flow direction matrix, (c) represents a detail of the computational scheme of the model related to water quality modeling and (d) represents the computational mesh, where the water quality states of the time a posteriori depends on the states of the neighboring cells and the time to the prior time-step. Furthermore, pollutant flow rates depend on the flow rate Q_{dir} for each direction. These flow rates are a function of the hydrodynamic model.

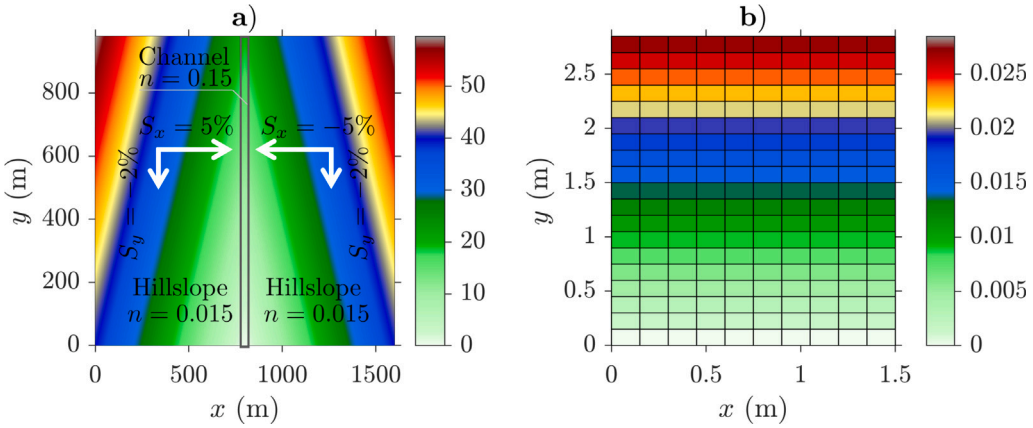

Fig. 4. Catchments of Numerical Case Study 1 and 2. Part (a) is the V-Tilted Catchment Digital Elevation Model (m), with smoother hillslopes and a rougher central channel. The outlet boundary condition is assumed as normal depth with slope of 0.02. The pixel dimension is 20 m. Infiltration is not modeled and the rainfall is spatially and temporally uniform with 10.8 mm h^{-1} during 90 min. Part (b) is the Wooden-Plane catchment digital elevation model (m) (Zhang et al., 2020) with pixels of 0.15 m with time and space invariant rainfall, and slope (s_0) of 1°, although it varies for some events assessed further. The outlet boundary condition of normal slope following the plane slope is assumed. Infiltration is also neglected, and an initial solute mass of 125 g is uniformly distributed in the catchment.

63.81 and 76.34 mm h^{-1}, respectively. Events 5 to 8 have slopes of 2° and rainfall intensities of 20.76, 41.72, 78.26 , 83.99 mm h^{-1}, respectively. From these 8 events, we perform a single calibration and validation test for each slope. For events 1 to 4 (i.e., $s_0 = 0.5°$), we select event 4 for calibration and the remainder for validation. In addition, for events 5 to 8 (i.e., $s_0 = 2°$), event 7 was used for calibration and the others for validation. To this end, we develop a calibration optimization problem minimizing the root-square mean error (RMSE)

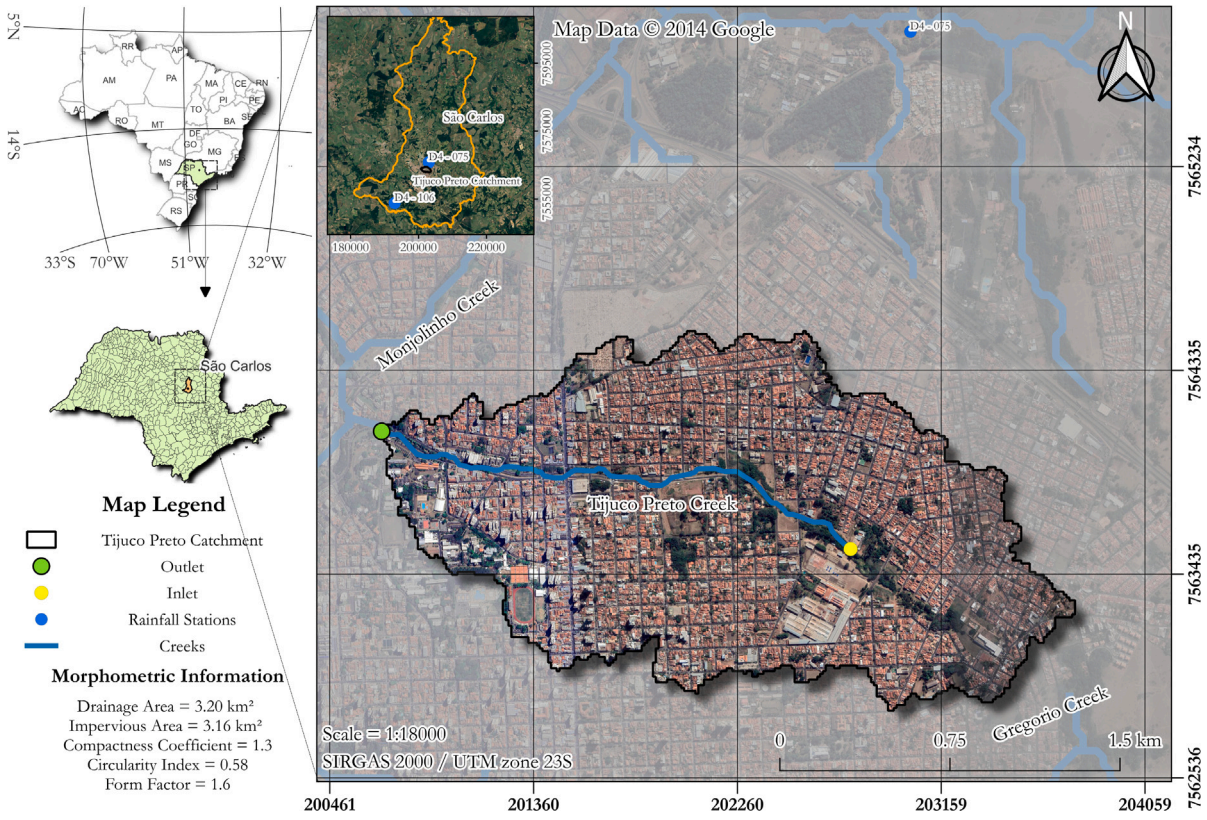

Fig. 5. Tijuco Preto catchment located in São Carlos - SP.
Source: Map data.
© 2015 Google and IBGE.

between modeled and observed salt concentrations. This procedure is fully described in the Supplemental Material. The decision variables for the optimization problem are the wash-off coefficients C_3 and C_4 and the problem is solved with the genetic algorithm for a 40 generation and population size of 100. The build-up coefficients C_1 and C_2 were not used in the calibration since the initial mass of salt is known.

2.4. Numerical case study 3 — The Tijuco Preto catchment in São Carlos – S/Brazil

The third case study tested the HydroPol2D model in the Tijuco Preto catchment (TPC), in São Carlos - São Paulo. The TPC is characterized by 95% of impervious areas (Baptista et al., 2021). The digital elevation model (DEM) was built based on elevation data with horizontal and vertical spatial resolution of 12.5 and 1 m, respectively, obtained from the Alos database Palsar (Rosenqvist et al., 2007). The LULC raster was obtained from the mapbiomas project, available at Souza et al. (2020) and was later reclassified into two main land uses: impermeable and permeable surfaces. Subsequently, a downscaling procedure was performed, using the nearest-neighbor method, on these data from 30 m to 12.5 m of horizontal resolution to match the DEM spatial resolution. Despite possible errors due to data resampling, this procedure is justified because the Alos Palsar data are the product of resampling the SRTM data from 30 to 12.5 m. Furthermore, the delineation of flood inundation maps with a resolution of 12.5 m provides a better level of detail in the modeling outputs, as it allows the capture of the flow path of streets and avenues.

This case of study is located in São Carlos - Brazil, which has experienced intense urbanization in recent decades (Ohnuma and Mendiondo, 2014). This catchment is comparable in characteristics of many highly urbanized catchments with a lack of high-resolution data on rainfall, elevation, and almost an absence of water quantity and quality observations.

The modeling efforts presented here aim to explain the transport phenomenon of TSS mobilized only as a function of surface runoff. TSS was chosen due to its good representation of the general state of water quality (Di Modugno et al., 2015; Rossman and Huber, 2016). To this end, the modeling of maximum water depths, maximum pollutants concentrations, and potential pollutant retention is evaluated. The TPC is shown in Fig. 5.

Despite the absent monitored data in this catchment, both in terms of high-resolution precipitation (e.g., sub-hourly intervals) and in terms of water depths or flows observed in the stream, the objective of this case study is to quantify in probabilistic terms the expectation of specific water depths of flood inundation depths, flow discharges, concentrations, and pollutant loads in pixels of the catchment, especially at the outlet. The rainfall on the grid boundary condition is a design spatially-invariant storm hyetograph distributed with the Alternated Blocks method (Keifer and Chu, 1957).

2.4.1. Probabilistic distribution of daily rainfall and antecedent dry days

For the maximum annual dry days and the subsequent creation of the ADD curve for the TPC, rainfall data was sought in the website of the Hydrological Database of the Department of Water and Electricity (DAEE), available at Prodesp (2022). The rainfall station with prefix D4 – 075 (see Fig. 3), named “São Carlos – SAAE”, located in the geographic coordinates 21°59′12″S, 47°52′33″W was chosen. However, this station lacks rainfall data between 1996 and 2013, and, in this case, we used the station *D*4 – 106, named “Fazenda Santa Bárbara” - located at coordinates 22° 05’38”S, 47° 58’30”W.

To estimate the maximum annual dry days in the TPC, data from station *D4*–075 were used between 1970 and 1995, and for the years 2014 to 2018. For the period from 1996 to 2013 and 2019, station *D*4 – 106 was

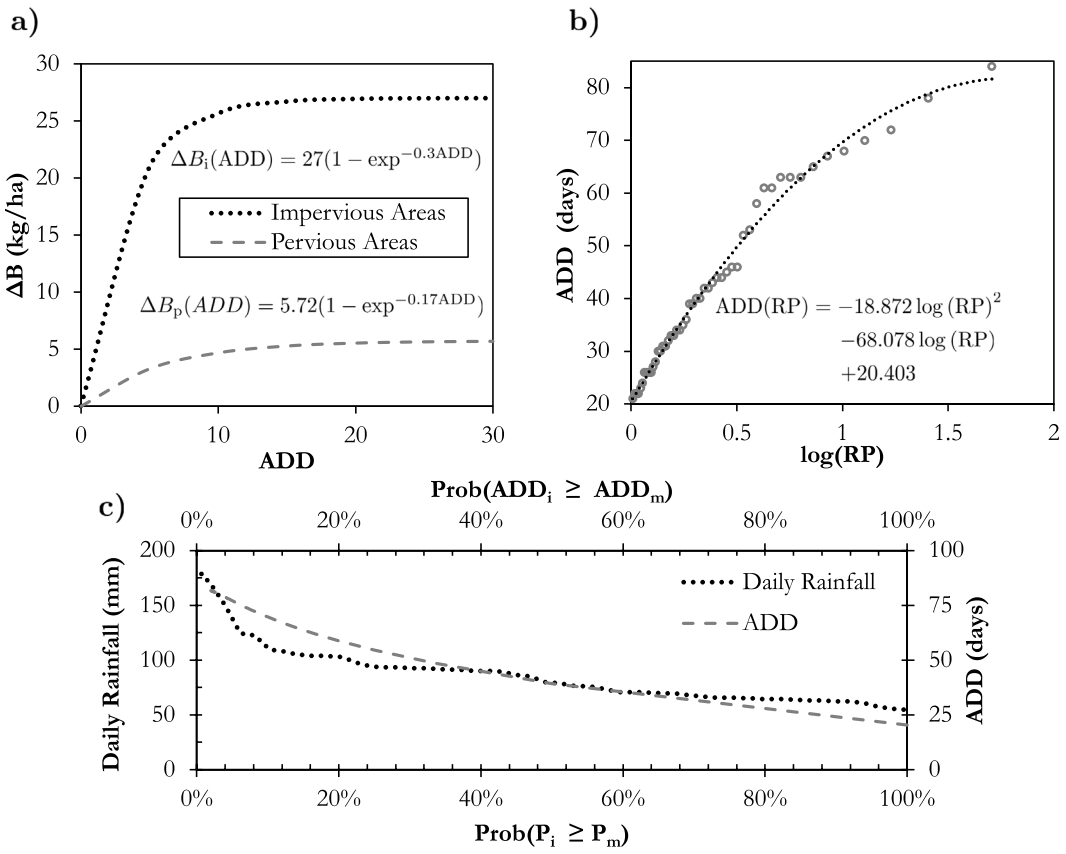

Fig. 6. Accumulation of pollutants (build-up) as a function of the interval of dry days (ADD), (b) Adjustment of dry days concerning empirical return periods simulated by the Weibull relation, and (c) Probability distribution of ADD and daily rainfall. The rainfall is assumed space invariant in the catchment.

used. Both stations do not have data for May 2016, so this year was not used for the analysis. It is observed that the expected values of ADD are on the order of 25 days for a *RP* of 1 year. The daily rainfall data presented in Fig. 6 were obtained from the DAEE platform and used to fit an updated IDF curve for São Carlos (Gomes Jr., 2019), with Sherman-type parameters of $K = 819.67$, $a = 1.388$, $b = 10.88$, and $c = 0.75$.

2.4.2. DEM treatment and reconditioning

Raw elevation information contains noise, accumulation points, depressions, and plateaus due to the low accuracy of the data. The elevation data was subjected to sequential processes to refine the hydraulic pathways in the catchment. First, a slope-based filter was used to remove possible noise from the elevation data, generating a raster that contains the terrain without peaks with a slope greater than 30° (*DTM filter* - SAGA (Passy and Théry, 2018)). This slope represents an elevation difference of 7.21 m between the boundary cells and the cells and could represent urban features such as buildings that should be removed from the terrain model. After this operation, a raster is generated with several areas left without data, and, in the absence of such data, a bilinear interpolation filter was used to smooth the terrain lines (*r.fillnuls* – GRASS (Lacaze et al., 2018)). This process ensures smoother flow lines. The final product of the procedure is shown in Fig. 7.

2.4.3. Warm-up process and initial values for modeling

In HydroPol2D, users can enter initial maps of water surface depths, pollutant mass, or enter a constant value per land use and land cover classification as warm-up data. In this paper, we performed a water quantity and quality warm-up by subjecting the catchment domain to an inflow hydrograph 0.3 $m^3\ s^{-1}$ for 24 h followed by a rain on the grid boundary condition with return period of 1-yr and 1-hour duration with the Alternated Blocks rainfall distribution. The pollutant initial build-up were estimated for a return period of 1/12 years, representing the available TSS mass in the catchment with RP, which results in ADD of 10 days. More details of the warm-up process can be found in the Supplemental Material.

2.4.4. Composite design event

The event simulated in this study corresponds to a combination of two consecutive events: frequent annual drought (e.g., RP = 1 year) followed by frequent annual rainfall (e.g., RP = 1 year). Thus, the return period of the composite event, which corresponds to the product of each RP event, also results in RP = 1 year. This design event was chosen because it represents a common event in the catchment in terms of both the accumulation of pollutants and the volume of precipitation. Furthermore, more frequent rainfall events tend to produce higher average concentrations because they carry a higher amount of pollutants in a smaller volume of surface runoff (Di Modugno et al., 2015). On the other hand, very frequent events (e.g., RP < 1/12 years) might not even produce surface runoff to carry pollutants. The base parameters assumed in the simulation were obtained based on the literature and studies such as Zaffani and Mendiondo (2012) for the TPC, presented in Table 2.

2.4.5. Parameter estimations and local sensitivity analysis

The absence of monitoring makes the formal calibration and validation of the model intractable. The parameters of the water quantity model were assumed a priori, based on satellite information on the catchment and inspections on site. The Manning coefficient and the losses by abstraction were assumed on the basis of the land use and land cover of the catchment, classified as permeable and impermeable. Since the catchment is almost entirely impermeable (i.e., there are relatively few losses through infiltration), the calibration of the hydrodynamic model would only consider the Manning's coefficient if we neglect the effect of the initial abstraction in impermeable areas. The assumed val-

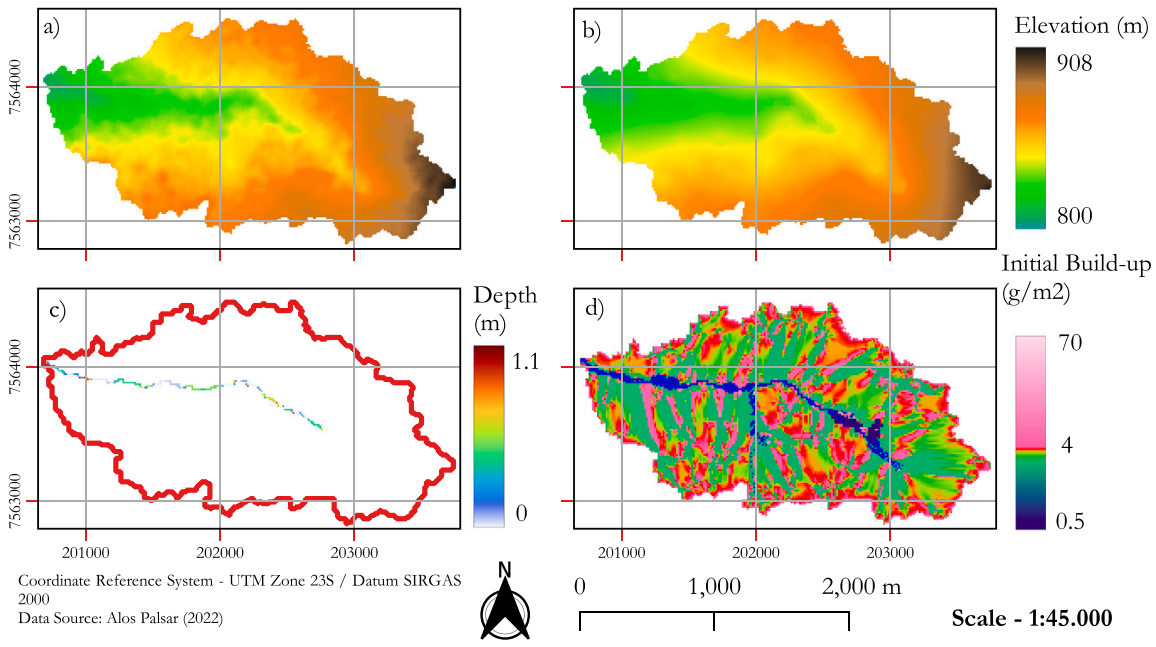

Fig. 7. Relationship between the original DEM and the reconditioned DEM developed to ensure hydrological continuity and warm-up data. Part (a) is the original elevation data, (b) is the reconditioned DEM, (c) is the warm-up depth, and (d) is the initial TSS mass (initial build-up).

Table 2
Parameters of the base scenario adopted in the simulation.

Land use classification	Parameters							
	k_{sat} (mm h^{-1})	$\Delta\theta$ (cm^3 cm^{-3})	n (s $m^{-1/3}$)	h_0 (mm)	C_1 (kg ha^{-1})	C_2 (day^{-1})	C_3 –	C_4 –
Impervious Areas	0	0	0.018	10	27.6	0.2	1200	1.2
Pervious Areas	10	0.4	0.100	20	5.72	0.17	1200	1.2

ues of the Manning's coefficient are twofold: one that represents impermeable areas and other that represent shrub and grass, since we have 2 land use and land cover classification in the catchment (Chow, 2010). For the water quality wash-off parameters, we perform a first estimate based on the scarce observations presented in Ohnuma and Mendiondo (2014). Furthermore, we evaluate the uncertainty in the wash-off parameters by a local sensitivity analysis varying the parameters +40% to −40% in terms of loads, concentrations and EMC of TSS.

In addition, we compared the HydroPol2D model with the HEC-RAS 2D full-momentum Pardiso fully implicit numerical solver (Brunner, 2016; Gomes Jr et al., 2023) to check the ability of the model to predict hydrographs at the outlet. In this analysis, we simulate the same design event but without infiltration and the initial abstraction effect.

2.5. Performance indicators

The performance indicators are used to evaluate the modeling prediction capacity of HydroPol2D for water quantity and water quality estimation. In this paper, we use the Nash-Sutcliffe-Efficiency (Nash and Sutcliffe, 1970), the coefficient of determination, the Root-Mean-Square-Error (Fisher et al., 1920), and the PBIAS (Neyman and Pearson, 2020). The equations of each indicator are detailed in the Supplemental Material.

3. Results and discussions

3.1. Numerical case study 1: The role of velocity limitation and numerical stability

The mathematical model is developed by numerical discretization of differential equations solved by explicit finite differences in a forward Euler fashion. Thus, this case study aims to assess the impact of different temporal discretization on the hydrodynamic modeling of the V-Tilted Catchment, typically used to assess the performance of hydrologic and hydrodynamic models. In this analysis, several time steps were used to evaluate the numerical validation of the solution considered, limiting or not limiting the velocity to the critical velocity. Since we use forward Euler's discretization method, care must be taken to select the proper computational temporal meshgrid because the method is unconditionally unstable. In this section, we compare several hydrographs with constant time-step, with guaranteed stability and evident instability, with simulations made using the adaptive stable time-step scheme, as illustrated in Fig. 8.

The different computational meshes used in the model reveal that the surface runoff modeling is practically invariant to cases where stable time-steps are chosen (see parts b and c in Fig. 8). This implies that once the CFL conditions are verified; the model can accurately predict hydrographs at the catchment outlet. The same is not true when we choose time-steps greater than 20 s. The system starts to show divergences from this value for both HydroPol2D models (a) and (b), generating a total loss of accuracy and numerical instability of the method for a time-step of 1 min.

Significant differences occur when the HydroPol2D model restricts its maximum wave velocity. Although theoretically neglecting the hydraulic regime change would mean relatively smaller velocities and, therefore, allow longer time-steps, it is not consistent with the reality of more intense flow phenomena, especially in the case of large floods with high velocities. In these cases, the modeling allowing regime switching is closer to the results simulated with the GSSHA, assumed as the base scenario in this case study. Both HydroPol2D models (a) and (b) accurately predicted the peak flow; however, only model (a) was able to capture the time to peak more precisely, as it did not

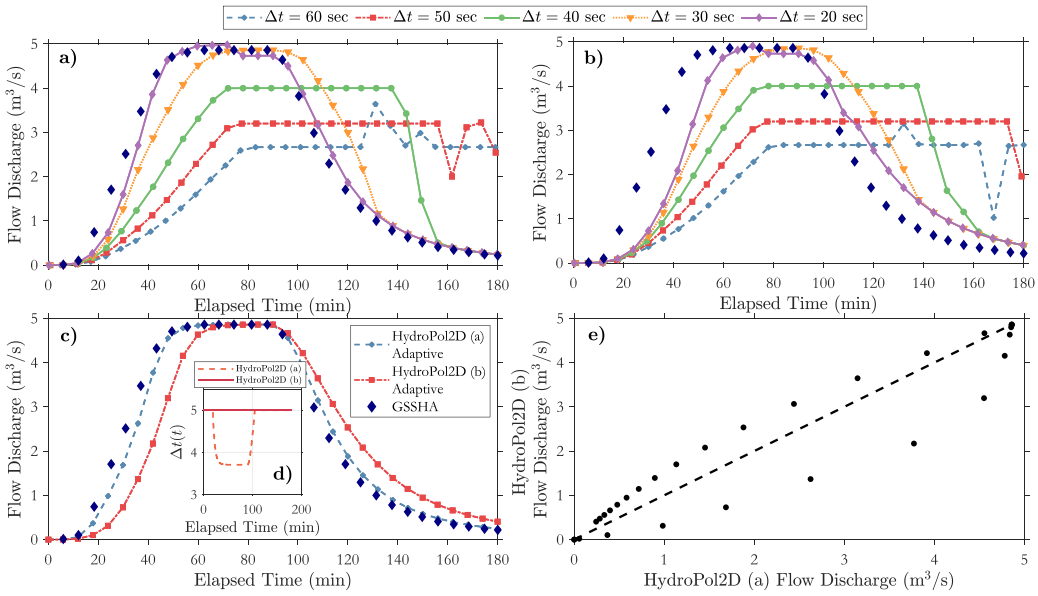

Fig. 8. Comparison of hydrographs generated by different computational meshes; where (a)–(b) represent hydrographs for simulated for unstable meshes. Part (a) represents unstable meshes of HydroPol2D (a) while part (b) represents unstable meshes of HydroPol2D (b). Part (c) shows GSSHA results compared with stable results of HydroPol2D (a) and (b) with adaptive time-step, with the time-steps presented in Part (d). Finally, part (e) shows a scatter plot of stable meshes of HydroPol2D (a) and (b).

limit the flow velocity. The HydroPol2D model (b) is identical to the model proposed by Guidolin et al. (2016), except that the HydroPol2D model allows one to calculate infiltration, water quality, and simulate different uses and land covers.

3.2. Numerical case study 2: Water quality model validation

The results of the numerical calibration are presented in detail in the Supplemental Material. The pollutographs of all eight events simulated with the statistics of RMSE, NSE, r^2, and PBIAS are presented in Fig. 9. The temporal dynamics of the solute was properly captured by the HydroPol2D model. The resulting calibrated parameters for events 1–4 are C_3 = 9036.83 and C_4 = 0.2435, while for events 5–8, C_3 = 7445.11 and C_4 = 0.1916. Although HydroPol2D can accurately capture the dynamics of the solute, calibration of water quality parameters is required and varies according to the physiographic characteristics of the catchment, such as slope, length, width, and roughness (Xiao et al., 2017; Zhang et al., 2020).

3.3. Numerical case study 3: Dynamics of water quantity and quality in poorly gauged catchments

3.3.1. Comparison between HEC-RAS and HydroPol2D

The results indicated in Fig. 10 show the goodness of fitness between HydroPol2D and HEC-RAS 2D in the Tijuco Preto catchment compared to the HydroPol2D model. The NSE index is 0.97, the r^2 is 0.98 and the PBIAS is 4.4%, indicating a good agreement between both models for all evaluated metrics.

3.3.2. Local sensitivity analysis

Although the parameter estimates are based on previous studies (Ohnuma and Mendiondo, 2014), a local sensitivity analysis was carried out to identify the most sensitive parameters in the water quality model. Fig. 11 (a) shows the sensitivity of C_3, which was more sensitive to changes in maximum concentration. However, the results of Fig. 11 (a) indicate that the wash-off coefficient (i.e., the ratio between the washed mass and the initially available mass) was not very sensitive to this variation, suggesting that the error in this parameter does not have a large effect on the total washed mass at the outlet. Both the EMC and the maximum load had a low sensitivity to C_3, indicating that its error does not compromise the average and diluted analyzes (e.g., EMC), but the dynamic ones such as the maximum concentration.

The results presented in Fig. 11 (b) show an opposite scenario than that shown in Fig. 11 (a). However, in general, decreasing C_4 increases peak concentrations and loads, which is explained by a greater mass swept at flow rates smaller than 1 m^3 s^{-1}(see Eq. (8)). Since the wash-off is a flow-dependent rating curve, lower C_4 exponents at flows lower than unity (i.e., 1 m^3 s^{-1}) increase the washed rates. Thus, larger masses washed in smaller volumes tend to increase the concentration. This is a numerical characteristic of the wash-off model used in this article. Another mathematical alternative to pollutants that do not follow the proposed rating curve is to add a factor μ to the flow, so that the flow used in the modeling of pollutants is $(Q + \mu)$, in order to avoid this numerical problem.

The maximum load rates of TSS increase with increasing C_4, indicating a higher instantaneous washing rate at the outlet in a given time. However, these loads occur only at large flows greater than unity; therefore, the increase in C_4, despite increasing the maximum load, decreases the wash-off coefficient because most flows are smaller than 1 m^3 s^{-1}. This implies that higher values of C_4 work well on heavy pollutants mobilized in large flows; however, as pollutants are mobilized only in large flows, the total mass washed is less than a case of lower C_4. On the basis of this same hypothesis, C_4 is concluded to have a strong relationship with the density and mean diameter of the pollutant.

Fig. 11 (c) presents the first-flush curve for each scenario evaluated. The critical cases of the first flush (that is, larger masses washed in smaller volumes) are more evident in the variation of C_3 (scenarios 1, 2, 3). In all cases except for scenario 8, more than 60% of the pollutants were washed with 30% by volume (Di Modugno et al., 2015), indicating a strong first-flush. This implies that even with eventual changes in the wash-off parameters, the first flush effect is mostly observed as a result of the high impervious rate of the catchment, which quickly washes the pollutants toward the outlet. The pollutograph showed high variability, as shown in Fig. 11 (d), with higher peaks for higher values of C_4 and C_3.

Therefore, if we consider a maximum uncertainty of 40% in the water quality parameters, Fig. 11 (c and d) would represent first-flush and pollutogram envelopes for the simulated event. Statistically, this

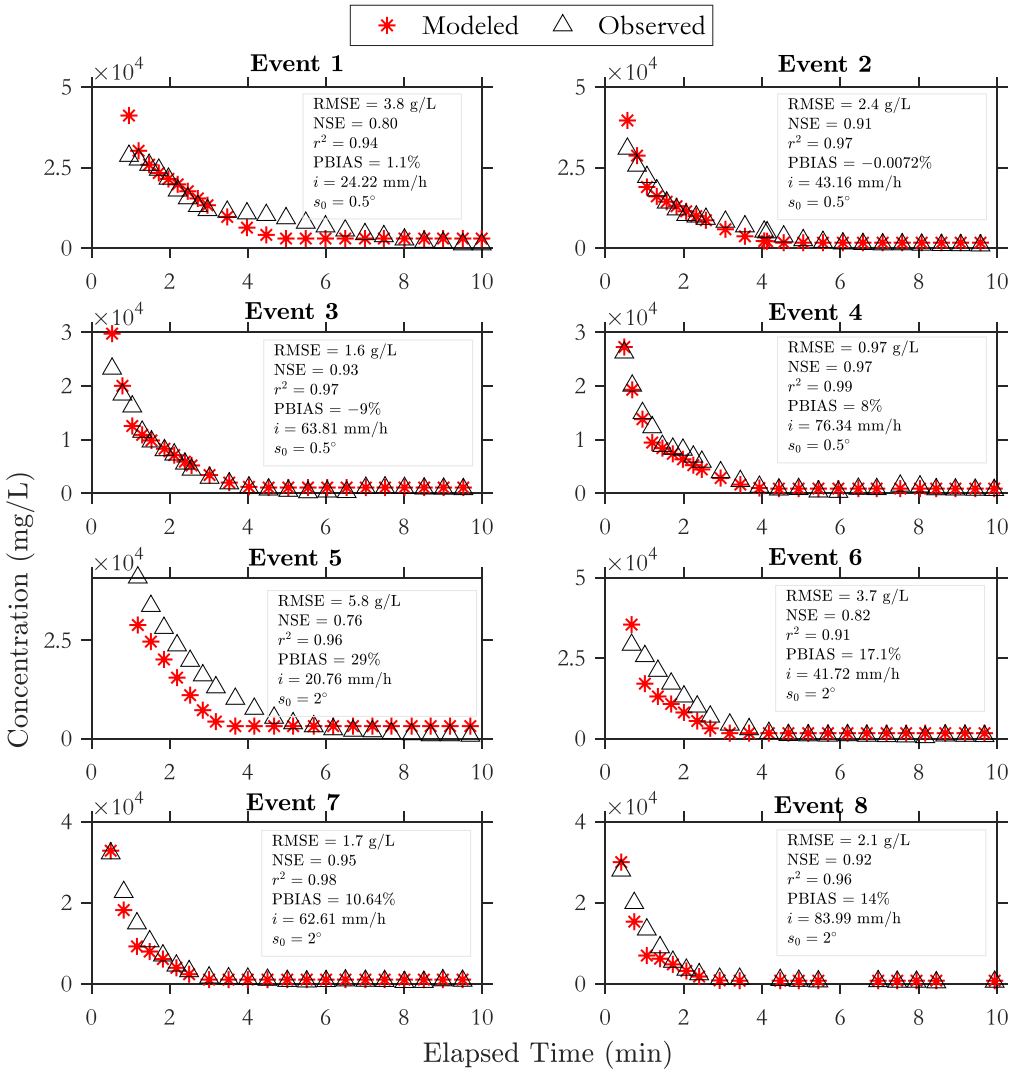

Fig. 9. Comparison between HydroPol2D pollutographs with observed concentration of salt in a laboratory wooden board catchment of 4.5 m^2 (Zhang et al., 2020). The initial mass of salt is 125 g and is uniformly distributed.

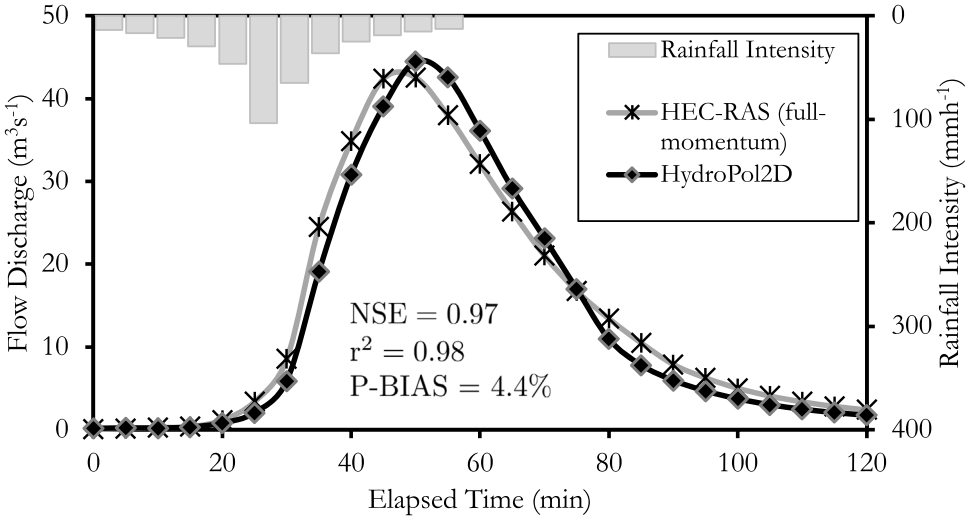

Fig. 10. Outlet hydrograph comparison between the full momentum solver used in HEC-RAS and the diffusive-like numerical solution approach used in the HydroPol2D model. Both outlet boundary conditions were assumed as normal depth with gradient slope of 2% and the catchment hydrological processes were simulated without infiltration and initial abstraction.

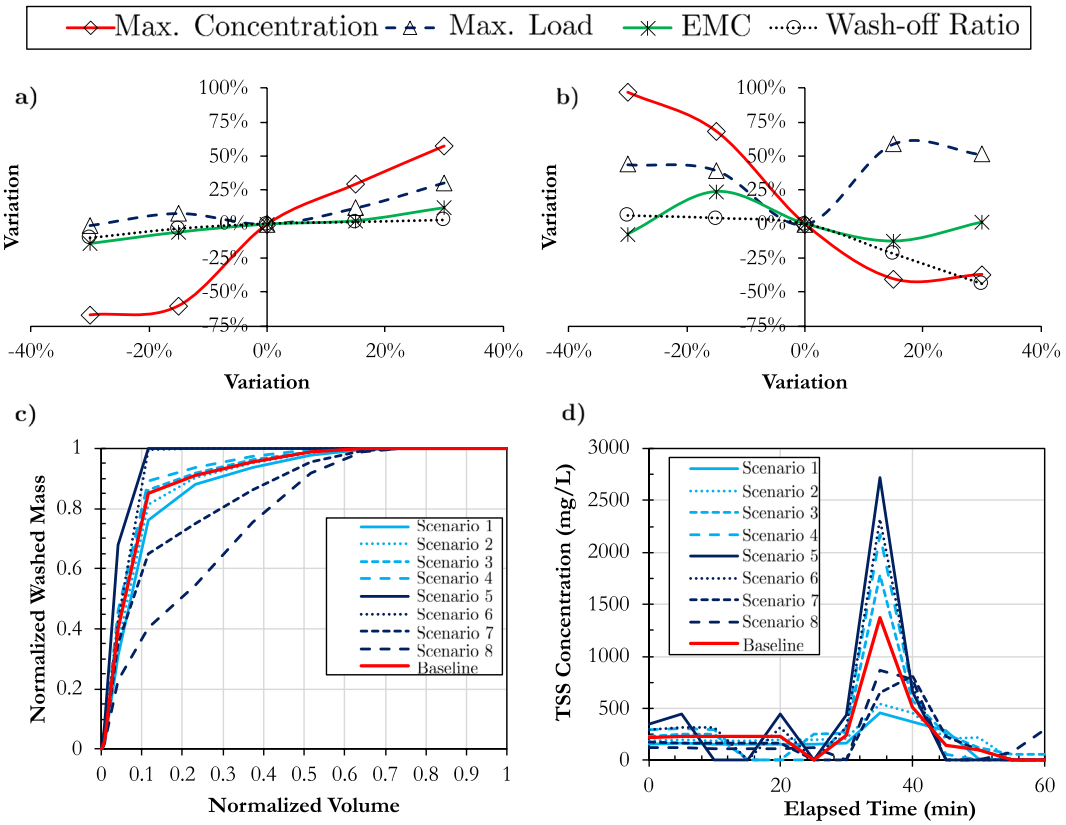

Fig. 11. Results of the model sensitivity analysis for an event of RP = 1 year, C_3 = 1,200 and C_4 = 1.2. Parts (a) and (b) represent the sensitivity of the maximum concentration, maximum load, and average concentration of the event for variations of C_3 (a) and C_4 (b). Parts (c) and (d) represent the first-flush curves and pollutographs of each simulated scenario, detailed in Table 3. The wash-off ratio is defined as the ratio between the washed mass and the available mass in the catchment.

Table 3
Data used in the sensitivity analysis and its respective modeling results.

Scenario	C_3	C_4	Maximum instantaneous concentration (mg L^{-1})	Maximum load (kg h^{-1})	EMC (mg L^{-1})	Washoff-Ratio
1	840	1.2	455.19	6.25	112.55	0.62
2	1020	1.2	548.33	6.81	123.83	0.67
3	1380	1.2	1786.73	7.06	135.18	0.70
4	1560	1.2	2174.31	8.22	148.11	0.71
5	1200	0.84	2716.02	9.09	121.85	0.74
6	1200	1.02	2319.25	8.81	163.13	0.72
7	1200	1.38	817.91	10.04	114.81	0.54
8	1200	1.56	862.95	9.55	133.29	0.39
Baseline	1200	1.2	1377.75	6.31	131.81	0.69

indicates that in 30% of the volume, 89% ±10% of the TSS of the catchment is swept away. Similarly, the maximum load and the maximum concentration of TSS are 8.22 ± 1.29 kg s^{-1} and 1,460 ± 832 mg L^{-1}, respectively, and the wash-off coefficient and EMC are 0.63 ± 0.11 and 131.59 ± 16 mg L^{-1}, respectively. Normalizing these values by the catchment area, the Load = 2.56 ± 0.4 kg s^{-1} km^{-2}, TSS = 456 ± 260 mg L^{-1} km^{-2}, EMC = 41 ±5 mg L^{-1} km^{-2}. These values are within the expected values for moderate rainfall in urbanized areas (Rossman and Huber, 2016).

3.3.3. Simulation results for RP = 1 year

The simulation of the TPC for 1 year return period event for rainfall and for the number of dry days is shown in Fig. 12. Fig. 12 (b) shows the maximum flood depth in the catchment, identifying areas susceptible to flooding with maximum depths of up to 1.50 m for an 1 hour of rainfall and 32 mm of volume distributed in Alternated Blocks. Fig. 12 (a) shows the maximum velocity map, which exceeded 10 m s^{-1} in the stream. Note that the maximum velocities are not necessarily associated with this maximum depth due to the rise and recession of the hydrographs with the propagation of the diffusive wave. The surface runoff generated was approximately equal to the total rainfall volume of 32 mm, except for the volume infiltrated in permeable areas, illustrated in Fig. 12 (e). In this figure, it is possible to observe infiltrated volumes greater than the precipitated volume. This occurred because the pervious areas receive runoff volume from several cells upstream, which increases the ponding depth and therefore increases the infiltration capacity. Although most of the catchment is impervious, flood depths occurred mainly in the stream, falling toward the overbanks only in a few areas, as illustrated in Fig. 12 (b). This occurred due to the relatively low return period assumed in the modeling.

Regarding the TSS transport, Fig. 12 (d) shows how much pollutants have flowed to each cell during the event studied. Naturally, the stream is the area with the greatest passage of pollutants. However, it is

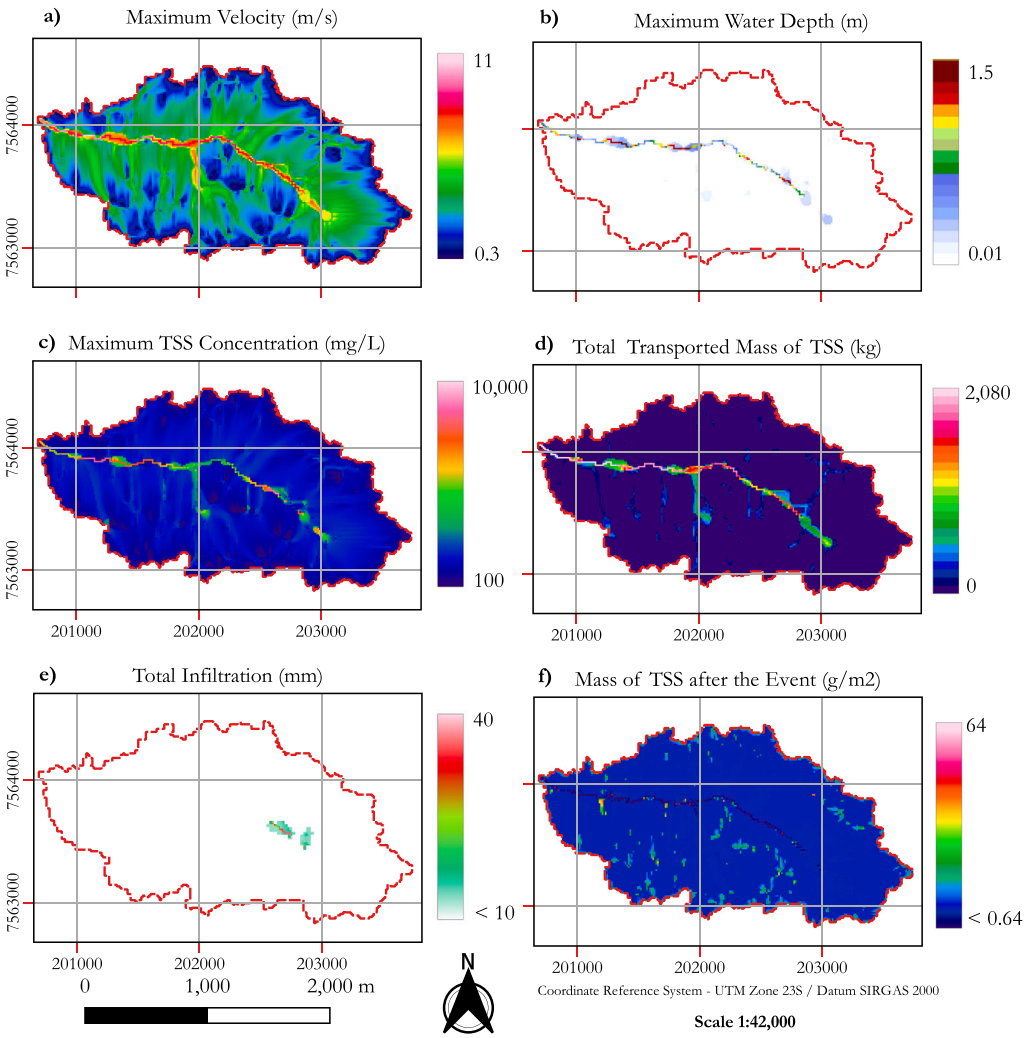

Fig. 12. Simulation results with baseline scenario parameters, where (a) is the maximum velocity, (b) is the map of maximum depths, (c) the maximum instantaneous concentration of TSS, (d) is the map that represents the total mass that passed through each cell. The catchment boundaries are given by the red dashed lines.

possible to identify locations outside the urban stream that also have a high level of pollution transport. These results could be strategically used to identify possible candidate areas for the implementation of LIDs. Therefore, this methodology makes it possible to quantitatively identify the most suitable areas to maximize the capture of pollutants carried by surface runoff, especially the TSS.

After the rainfall event, the remaining mass in the catchment is shown in Fig. 12 (f). This map illustrates the relatively clean stream and some areas with a relatively large accumulation of pollutants (e.g., > 60 g m^{-2} or 9.3 kg of TSS in each pixel of 156.25 m^2). Therefore, this map can help identify areas of accumulation and can serve as information for model calibration when used for sediment modeling. Despite being more dynamic and instantaneous, the maximum concentration also allows one to identify the maximum polluting potential of surface runoff water, as illustrated in Fig. 12 (c).

The analysis of the normalized outlet hydrograph result is presented in Fig. 13. It is possible to observe the hysteresis phenomenon (Aich et al., 2014), which shows that the concentration peak occurs approximately 25 min before the surface runoff peak. First, the rainfall peak occurs, following the concentration, load, and discharge peak, respectively. The first flush chart also shows that more than 90% of the TSS are washed in 30% of the volume. The same chart allows us to estimate (i) the time of concentration for this event, (ii) the peak time of flow discharges, concentrations, and loads, and allows comparison of results with other catchments, since all values are normalized by the catchment area.

3.4. Challenges and limitations of the application of distributed models in poorly-gauged catchments

Depending on the purpose and scale of the study, elevation data may be crucial in applying hydrological and water quality models. In the case of modeling focused on the delineation of flood inundation maps, FEMA, the Federal Emergency Agency of the United States, recommends as a minimum criterion hydrodynamic simulations with a resolution of up to 3 m with a vertical resolution of at most 1 cm. Detailed elevation data are available in countries such as Brazil only in some large cities, e.g. São Paulo, making it difficult to apply them at several important points where floods occur (Santos et al., 2016).

The most recurring application of hydrodynamic models is the study and delineation of flood inundation areas (do Lago et al., 2021; Erena et al., 2018; Fava et al., 2022). Although the HydroPol2D model does not solve the complete Saint-Venant 2D equations, its diffusive wave methodology is promising for determining flood areas in catchments where convective and local acceleration phenomena do not act as the main hydrodynamic governing processes. The flood inundation depth coupled with the velocity maps can serve as a basis to calculate the risk of human instability during a flood event (Rotava et al., 2013), to assess potential flood damage (Jamali et al., 2018) or as input data for estimating the value of flood insurance policies (Aerts and Botzen, 2011). Furthermore, the model can be used to estimate the time of concentration without requiring calculating it by empirical formulae (Manoj et al., 2012), as previously presented. Additionally,

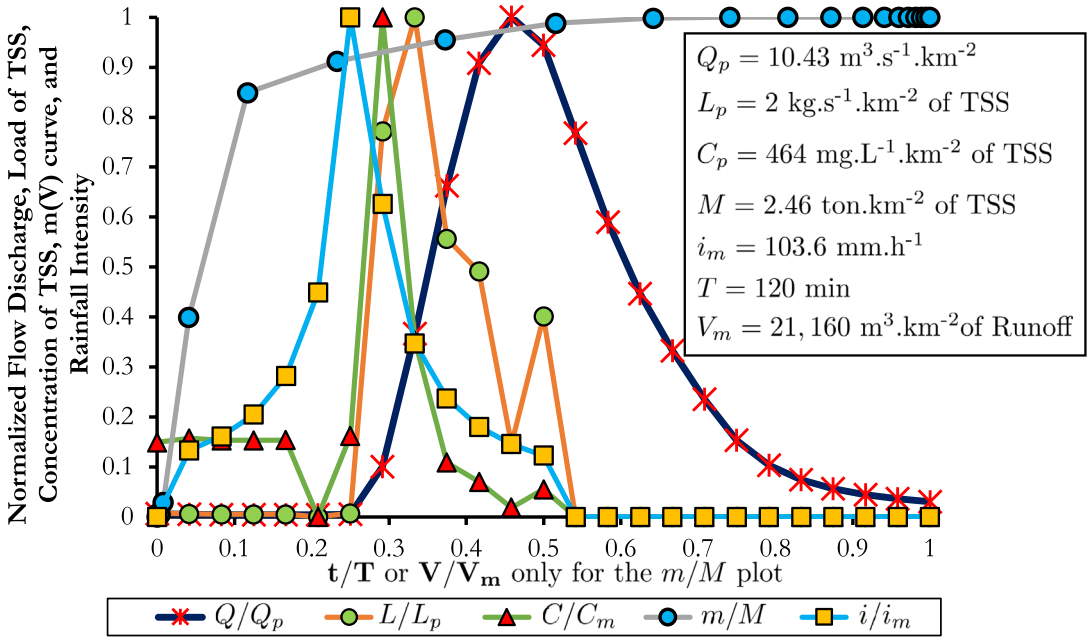

Fig. 13. Normalized modeling results, where all values are divided by their next maximum values and are typically divided by the watershed area of 3.20 km^2. Q is the flow discharge, Q_p is the peak flow, L is the pollutant load, L_p is the maximum pollutant load, C is the pollutant concentration, C_p is the maximum pollutant concentration m is the washed pollutant mass, M is the total mass of pollutant washed, i is the rainfall intensity, i_m is the maximum rainfall intensity, t is the time and T is the total duration.

flows at the catchment outlet can be estimated without the need for unit hydrographs.

Examples of the use of distributed models to determine hydrographs are presented in Furl et al. (2018), Sharif et al. (2010) and Sharif et al. (2013). To this end, however, if the information on where the stream passes is dissolved in the coarse resolution of the elevation pixels, it is necessary to recondition the terrain model, smoothing thalweg lines and elevation peaks, or sometimes imposing lower elevations in channel sections as presented in this paper. Another application is the spatial assessment of infiltration, which can be important in some urban areas and plays a major role in rural areas. This analysis can aid in spatial quantification of infiltration, which can aid in the decision about the implanted or chosen crop (Paudel et al., 2011). These examples show that, although modeling aimed at delineating flooded areas via 2D modeling requires high spatial resolution DEM, the determination of flows and, at least, the identification of critical points in the catchment can be identified with free data derived from satellite products (e.g., SRTM Drusch et al., 2012 and Alos Palsar Rosenqvist et al., 2007).

The most uncertain variable that is very difficult to estimate is the initial build-up map (Wijesiri et al., 2015b). Several studies indicate that the use of the build-up equation with ADD as a dependent variable may not correctly represent the pollutant accumulation process in urban catchments (Bonhomme and Petrucci, 2017; Zhang et al., 2019). Variables such as the predominant wind speed and direction, atmospheric pressure, humidity, and the geographic position of the catchment near roads and highways, among others, can play an essential role in the accumulation of pollutants (Pandey et al., 2016). Furthermore, the build-up model assumes a uniform accumulation for each land use, disregarding accumulation characteristics (e.g., source pollution release). All these limitations must be taken into account when modeling water quality. The HydroPol2D model, although developed for non-point source pollution, allows the modeling of source pollution by entering load rates at specific cells as external boundary conditions.

Despite the difficulties in model calibration, most parameters can be estimated, at least at the preliminary analysis level, based on the literature (Rossman et al., 2010). Sensitivity analysis reveals that the most important parameters of the model are the Manning's roughness coefficients and the wash-off coefficients, especially the exponent (C_4). Both parameters can be derived as a function of land use classifications. The model makes it possible to identify, using mostly physically-based equations, the hydrological, hydrodynamic, and distribution behavior of diffusive pollution in catchments where Hortonian processes govern the flow. The model allows for the estimation of important factors at the outlet level and spatialized values throughout the catchment. Therefore, one of the applications is to determine the critical areas of accumulation of pollutants in the catchment during and after precipitation events. This information can be used in master plans for better water quality management and to define potential areas to implement LID techniques focused on treating part of surface runoff (Batalini de Macedo et al., 2022; McClymont et al., 2020; de Oliveira et al., 2021).

Furthermore, the model can be used to evaluate the spatial impact of LIDs at the watershed scale by modeling its pixels with different land use and elevation properties (e.g., reducing the pixel elevation to simulate the ponding layer on the surface). This analysis can be done to quantify water quality and estimate the volumes of surface runoff retention. In addition, at the outlet of the catchment, dynamic factors such as the load and concentration of pollutants are estimated and are indicators of the response of the catchment to simulated events. Finally, the first flush modeling can be performed using the HydroPol2D model, which is an important evaluation for urbanized catchments.

4. Conclusions

Evaluating the impacts of surface runoff quality and quantity in urbanized catchments requires the temporal and spatial quantification of flood depths, pollutant transport, and fate. With this focus, the HydroPol2D model was designed and first applied in the V-tilted catchment to identify the role of the maximum flow velocity limitation. Our results indicates that limiting velocities to critical, reduce the model performance. The HydroPol2D water quality module was calibrated and validated with the observed data provided from a wooden board catchment. Subsequently, the model was applied in the Tijuco Preto catchment in São Carlos — focusing on the qualitative and quantitative quantification of the spatial–temporal behavior of surface runoff. Even with the lack of observed or high-resolution elevation data, it was possible to evaluate the quali-quantitative dynamics of the stormwater runoff for a return period of 1 year, both for rainfall and the number of antecedent dry days. An event composed of drought followed by a

flood was evaluated. The results of the numerical simulation for the Numerical Case Study 3 indicate the following:

- The maximum load and the maximum TSS concentration at the outlet are 8.22 ± 1.29 kg s^{-1} and $1,460 \pm 832$ mg L^{-1}. Normalizing by the catchment area of 3.20 km^2 it follows that the maximum concentration of TSS is 456 ± 260 mg L^{-1} km^{-2} and the maximum load of TSS is 2.56 ± 0.4 kg s^{-1} km^{-2} for a 1-yr flood–drought event.
- The Washoff-Ratio coefficient and the EMC were 0.63 ± 0.11 and 131.59 ± 16 mg L^{-1}, respectively, for a 1-yr flood–drought event.
- The volume of TSS washed in 30% of the runoff volume was $89\% \pm 10\%$, indicating a high first-flush phenomena in the catchment, considering an uncertainty in wash-off parameters from −40% to 40%.

The results of this article show how quali-quantitative modeling can be used to determine possible areas for applying LIDs, delineating areas prone to flooding, analysis of maximum flow velocities, and therefore risk of human instability due to floods. Furthermore, it allows to identify maps of maximum pollutant concentration. Despite the impossibility of calibrating the model for the TPC catchment due to lack of data, the calibration of quali-quantitative parameters is encouraged and can be done in the model via automatic calibration using optimization packages in Matlab (Higham and Higham, 2016). Furthermore, the analysis performed can be replicated for other combinations of RPs for rainfall and antecedent dry days. Future studies will incorporate resilience metrics, not only for short-term forecasts but also for scenario-based climate change predictions in large-scale watersheds. Thus, HydroPol2D can flexibly assess floods, drought-flood composite events, and water quality to aid decision-making in warning systems. Moreover, future work will incorporate modeling via continuous simulation. In this case, spatially varied climatological forcing and even drought-flood pooling under anthropic land-use change can be performed through HydroPol2D. Finally, testing the simulation computational time performance of the model against state-of-the-art software is also desired.

As in other distributed models, the challenge for the quality of the results presented by HydroPol2D is related to the quality of the input data, especially the topography and land use and land cover data. However, the model requires relatively few parameters to describe the hydraulic properties of the terrain and allows us to simulate quantity and/or quality. When simulating only water quantity, significant differences in processing time are obtained with HydroPol2D. Another advantage is the model's applicability, which, if the hydrological processes are predominantly Hortonian, allows simulating catchments at all spatial scales. Future studies will incorporate spatial variability of rainfall and evapotranspiration for large-scale watersheds, especially for modeling under periods of persistent droughts with unprecedented floods. Ultimately, the HydroPol2D model can become a tool for a wide range of purposes, either in real-time forecasting or even in scenarios under change, by incorporating distributed modeling of hydrodynamics and pollutant transport and fate.

CRediT authorship contribution statement

Marcus Nóbrega Gomes Jr.: Conceptualization, Methodology, Software, Validation, Formal analysis, Investigation, Data curation, Writing – original draft, Writing – review & editing, Visualization. **César Ambrogi Ferreira do Lago:** Writing – review & editing. **Luis Miguel Castillo Rápalo:** Writing – review & editing, Data curation, Resources. **Paulo Tarso S. Oliveira:** Writing – review & editing. **Marcio Hofheinz Giacomoni:** Writing – review & editing, Funding acquisition, Visualization, Resources. **Eduardo Mario Mendiondo:** Writing – review & editing, Funding acquisition, Visualization, Resources.

Declaration of competing interest

The authors declare that they have no known competing financial interests or personal relationships that could have appeared to influence the work reported in this paper.

Data availability

Algorithms and data used are available in an open repository at https://github.com/marcusnobrega-eng/HydroPol2D.

Acknowledgments

The authors appreciate the support of the City of San Antonio, by the San Antonio River Authority, United States of America, CAPES Ph.D Scholarship, Brazil, and the PPGSHS PROEX Graduate Program, Brazil. The authors also appreciate the support given by Grant # FAPESP 22/08468-0 "Flash drought event evolution characteristics and response mechanism to climate change", Grant # FAPESP 14/50848-9 "INCTMC2 Nat. Inst. of Sci. & Tech. for Climate Change Phase 2 Water Security Subcomponent, and Grant 139529Q/3281199 Univ Montpellier I-SITE Excellence Program, Campus France. We also express our gratitude to Dr. H. Khairourane, Prof. D. Cornu, Prof. P. Miele, Prof R. Pellenq, and Prof. Zaviska, for insightful discussions about "Urban Physics and Complex Cities".

Appendix A. Supplementary data

Supplementary material related to this article can be found online at https://doi.org/10.1016/j.jhydrol.2023.129982. Supplementary data related to this article can be found at https://github.com/marcusnobrega-eng/HydroPol2D.

References

Aerts, J.C., Botzen, W.W., 2011. Climate change impacts on pricing long-term flood insurance: A comprehensive study for the netherlands. Glob. Environ. Chang. 21 (3), 1045–1060.

Aich, V., Zimmermann, A., Elsenbeer, H., 2014. Quantification and interpretation of suspended-sediment discharge hysteresis patterns: how much data do we need? Catena 122, 120–129.

Arnold, J.G., Moriasi, D.N., Gassman, P.W., Abbaspour, K.C., White, M.J., Srinivasan, R., Santhi, C., Harmel, R., Van Griensven, A., Van Liew, M.W., et al., 2012. SWAT: Model use, calibration, and validation. Trans. ASABE 55 (4), 1491–1508.

Baptista, M.V., Scarpinella, G.D., Menezes, D.B., 2021. Idas e vindas do processo de degradação e recuperação de um córrego urbano. Simpósio Nac. Gestao Engenharia Urbana 3, 87–95.

Batalini de Macedo, M., Nobrega Gomes Junior, M., Pereira de Oliveira, T.R., H. Giacomoni, M., Imani, M., Zhang, K., Ambrogi Ferreira do Lago, C., Mendiondo, E.M., 2022. Low impact development practices in the context of united nations sustainable development goals: A new concept, lessons learned and challenges. Crit. Rev. Environ. Sci. Technol. 52 (14), 2538–2581.

Bonhomme, C., Petrucci, G., 2017. Should we trust build-up/wash-off water quality models at the scale of urban catchments? Water Res. 108, 422–431.

Brighenti, T.M., Bonumá, N.B., Srinivasan, R., Chaffe, P.L.B., 2019. Simulating sub-daily hydrological process with SWAT: a review. Hydrol. Sci. J. 64 (12), 1415–1423.

Brunner, G.W., 2016. HEC-RAS River Analysis System Modeling User's Manual US Army Corps of Engineers Hydrologic Engineering Center. Information on http://www.hec.usace.army.mil.

Chow, T., 2010. V (2010). Applied Hydrology. Tata McGraw-Hill Education.

Collischonn, W., Allasia, D., Da Silva, B.C., Tucci, C.E., 2007. The MGB-iph model for large-scale rainfall—runoff modelling. Hydrol. Sci. J. 52 (5), 878–895.

Courant, R., Friedrichs, K., Lewy, H., 1928. Über die partiellen differenzengleichungen der mathematischen physik. Math. Ann. 100 (1), 32–74.

de Oliveira, T.R.P., de Macedo, M.B., Oliveira, T.H., do Lago, C.A.F., Gomes, Jr., M.N., Brasil, J.A.T., Mendiondo, E.M., 2021. Different configurations of a bioretention system focused on stormwater harvesting in Brazil. J. Environ. Eng. 147 (12), 04021058.

De Paiva, R.C.D., Buarque, D.C., Collischonn, W., Bonnet, M.P., Frappart, F., Calmant, S., Bulhões Mendes, C.A., 2013. Large-scale hydrologic and hydrodynamic modeling of the Amazon River basin. Water Resour. Res. 49 (3), 1226–1243.

Deletic, A., 1998. The first flush load of urban surface runoff. Water Res. 32 (8), 2462–2470.

Di Modugno, M., Gioia, A., Gorgoglione, A., Iacobellis, V., La Forgia, G., Piccinni, A.F., Ranieri, E., 2015. Build-up/wash-off monitoring and assessment for sustainable management of first flush in an urban area. Sustainability 7 (5), 5050–5070.

do Lago, C.A., Giacomoni, M.H., Bentivoglio, R., Taormina, R., Junior, M.N.G., Mendiondo, E.M., 2023. Generalizing rapid flood predictions to unseen urban catchments with conditional generative adversarial networks. J. Hydrol. 618, 129276.

do Lago, C.A.F., Hofheinz Giacomoni, M., Olivera, F., Mario Mendiondo, E., 2021. Assessing the impact of climate change on transportation infrastructure using the hydrologic-footprint-residence metric. J. Hydrol. Eng. 26 (5), 04021014.

Downer, C.W., Ogden, F.L., 2004. GSSHA: Model to simulate diverse stream flow producing processes. J. Hydrol. Eng. 9 (3), 161–174.

Downer, C.W., Pradhan, N.R., Ogden, F.L., Byrd, A.R., 2015. Testing the effects of detachment limits and transport capacity formulation on sediment runoff predictions using the US Army Corps of Engineers GSSHA model. J. Hydrol. Eng. 20 (7), 04014082.

Drusch, M., Del Bello, U., Carlier, S., Colin, O., Fernandez, V., Gascon, F., Hoersch, B., Isola, C., Laberinti, P., Martimort, P., et al., 2012. Sentinel-2: ESA's optical high-resolution mission for GMES operational services. Remote Sens. Environ. 120, 25–36.

Erena, S.H., Worku, H., De Paola, F., 2018. Flood hazard mapping using FLO-2D and local management strategies of dire dawa city, ethiopia. J. Hydrol. Reg. Stud. 19, 224–239.

Fan, F.M., Collischonn, W., 2014. Integração do modelo MGB-IPH com sistema de informação geográfica. RBRH: Revis. Brasileira Recursos Hidricos. Porto Alegre, RS 19 (1), 243–254.

Farooq, M., Shafique, M., Khattak, M.S., 2019. Flood hazard assessment and mapping of river swat using HEC-RAS 2D model and high-resolution 12-m TanDEM-X DEM (worlddem). Nat. Hazards 97 (2), 477–492.

Fava, M.C., Macedo, M.B.d., Buarque, A.C.S., Saraiva, A.M., Delbem, A.C.B., Mendiondo, E.M., 2022. Linking urban floods to citizen science and low impact development in poorly gauged basins under climate changes for dynamic resilience evaluation. Water 14 (9), 1467.

Fisher, R.A., et al., 1920. 012: A mathematical examination of the methods of determining the accuracy of an observation by the mean error, and by the mean square error.

Fry, T.J., Maxwell, R.M., 2018. Using a distributed hydrologic model to improve the green infrastructure parameterization used in a lumped model. Water 10 (12), 1756.

Fu, B., Merritt, W.S., Croke, B.F., Weber, T.R., Jakeman, A.J., 2019. A review of catchment-scale water quality and erosion models and a synthesis of future prospects. Environ. Model. Softw. 114, 75–97.

Furl, C., Ghebreyesus, D., Sharif, H.O., 2018. Assessment of the performance of satellite-based precipitation products for flood events across diverse spatial scales using GSSHA modeling system. Geosciences 8 (6), 191.

Getirana, A.C., Boone, A., Yamazaki, D., Decharme, B., Papa, F., Mognard, N., 2012. The hydrological modeling and analysis platform (HyMAP): Evaluation in the amazon basin. J. Hydrometeorol. 13 (6), 1641–1665.

Gomes Jr., M.N., 2019. Aspectos hidrológicos-hidráulicos e avaliação da eficiência de biorretenções: modelos, princípios e critérios de projeto de técnicas compensatórias de 3ª geração. Universidade de São Paulo.

Gomes Jr., 2023. HydroPol2D v.0.0.1. GitHub repository, GitHub, https://github.com/marcusnobrega-eng/HydroPol2D.

Gomes Jr., M., Giacomoni, M., Papagiannakis, A., Mendiondo, E., Dornelles, F., 2021. Spatial assessment of overland flow, pollutant concentration, and first flush using a 2-D non-point source pollution and hydrological model for urban catchments. In: World Environmental and Water Resources Congress. pp. 397–413.

Gomes Jr., M.N., Giacomoni, M.H., Taha, A.F., Mendiondo, E.M., 2022. Flood risk mitigation and valve control in stormwater systems: State-space modeling, control algorithms, and case studies. J. Water Resour. Plan. Manag. 148 (12), 04022067.

Gomes Jr, M.N., Rápalo, L.M., Oliveira, P.T., Giacomoni, M.H., do Lago, C.A., Mendiondo, E.M., 2023. Modeling unsteady and steady 1d hydrodynamics under different hydraulic conceptualizations: model/software development and case studies. Environmental Modelling & Software 105733.

Green W. H, A.G., 1911. Studies on soil physics. J. Agric. Sci. 4 (1), 1–24.

Guidolin, M., Chen, A.S., Ghimire, B., Keedwell, E.C., Djordjević, S., Savić, D.A., 2016. A weighted cellular automata 2D inundation model for rapid flood analysis. Environ. Model. Softw. 84, 378–394.

Higham, D.J., Higham, N.J., 2016. MATLAB Guide. SIAM.

Hossain, I., Imteaz, M.A., Hossain, M.I., 2012. Application of a catchment water quality model for an East-Australian catchment. Int. J. Glob. Environ. Issues 12 (2–4), 242–255.

Jamali, B., Löwe, R., Bach, P.M., Urich, C., Arnbjerg-Nielsen, K., Deletic, A., 2018. A rapid urban flood inundation and damage assessment model. J. Hydrol. 564, 1085–1098.

Kabir, S., Patidar, S., Xia, X., Liang, Q., Neal, J., Pender, G., 2020. A deep convolutional neural network model for rapid prediction of fluvial flood inundation. J. Hydrol. 590, 125481.

Keifer, C.J., Chu, H.H., 1957. Synthetic storm pattern for drainage design. J. Hydraul. Div. 83 (4), 1332–1.

Knightes, C.D., Ambrose, Jr., R.B., Avant, B., Han, Y., Acrey, B., Bouchard, D.C., Zepp, R., Wool, T., 2019. Modeling framework for simulating concentrations of solute chemicals, nanoparticles, and solids in surface waters and sediments: WASP8 Advanced Toxicant Module. Environ. Model. Softw. 111, 444–458.

Kollet, S.J., Maxwell, R.M., 2006. Integrated surface–groundwater flow modeling: A free-surface overland flow boundary condition in a parallel groundwater flow model. Adv. Water Resour. 29 (7), 945–958.

Kreibich, H., Van Loon, A.F., Schröter, K., Ward, P.J., Mazzoleni, M., Sairam, N., Abeshu, G.W., Agafonova, S., AghaKouchak, A., Aksoy, H., et al., 2022. The challenge of unprecedented floods and droughts in risk management. Nature 608 (7921), 80–86.

Lacaze, B., Dudek, J., Picard, J., 2018. Grass gis software with qgis. QGIS Generic Tools 1, 67–106.

Lantz, R., 1971. Quantitative evaluation of numerical diffusion (truncation error). Soc. Petrol. Eng. J. 11 (03), 315–320.

Manoj, K., Fang, X., Yi, Y.J., Li, M.H., Cleveland, T.G., Thompson, D.B., 2012. Estimating time of concentration on low-slope planes using diffusion hydrodynamic model. In: World Environmental and Water Resources Congress 2012: Crossing Boundaries. pp. 360–371.

McClymont, K., Cunha, D.G.F., Maidment, C., Ashagre, B., Vasconcelos, A.F., de Macedo, M.B., Dos Santos, M.F.N., Júnior, M.N.G., Mendiondo, E.M., Barbassa, A.P., et al., 2020. Towards urban resilience through Sustainable Drainage Systems: A multi-objective optimisation problem. J. Environ. Manag. 275, 111173.

Melo, L.S., Costa, V.A., Fernandes, W.S., 2023. Assessing the anthropogenic and climatic components in runoff changes of the são francisco river catchment. Water Resources Management 1–15.

Nash, J.E., Sutcliffe, J.V., 1970. River flow forecasting through conceptual models part I—A discussion of principles. J. Hydrol. 10 (3), 282–290.

Neyman, J., Pearson, E.S., 2020. Contributions to the theory of testing statistical hypotheses. In: Joint Statistical Papers. University of California Press, pp. 265–297.

Ohnuma, Jr., A.A., Mendiondo, E.M., 2014. Análise de cenários com proposição de medidas de recuperação ambiental para a micro-bacia do Tijuco Preto, São Carlos-SP. Braz. J. Environ. Sci. (32), 42–51 (Online).

Pandey, A., Himanshu, S.K., Mishra, S.K., Singh, V.P., 2016. Physically based soil erosion and sediment yield models revisited. Catena 147, 595–620.

Passy, P., Théry, S., 2018. The use of SAGA GIS modules in QGIS. QGIS Generic Tools 1, 107–149.

Paudel, M., Nelson, E.J., Downer, C.W., Hotchkiss, R., 2011. Comparing the capability of distributed and lumped hydrologic models for analyzing the effects of land use change. J. Hydroinformatics 13 (3), 461–473.

Prodesp, 2022. DAEE. Portal Dep. Aguas Energia Eletrica URL http://www.hidrologia.daee.sp.gov.br/.

Richards, L.A., 1931. Capillary conduction of liquids through porous mediums. Physics 1 (5), 318–333.

Rosenqvist, A., Shimada, M., Ito, N., Watanabe, M., 2007. ALOS PALSAR: A pathfinder mission for global-scale monitoring of the environment. IEEE Trans. Geosci. Remote Sens. 45 (11), 3307–3316.

Rossman, L.A., Huber, W.C., 2016. Storm water management model reference manual. In: Volume III—Water Quality.

Rossman, L.A., et al., 2010. Storm Water Management Model User's Manual, Version 5.0. National Risk Management Research Laboratory, Office of Research and ....

Rotava, J., Mendiondo, E.M., Souza, V.C.B., 2013. Simulação de instabilidade humana em inundações: primeiras considerações. XX Simpósio Brasileiro Recursos Hídricos 1–8.

Santos, M.A., Carvalho, S.M., Antoneli, V., 2016. Suscetibilidade de enchentes a partir da análise das variáveis morfométricas na bacia hidrográfica rio bonito em Irati-PR-brasil. Revista Equador 5 (5), 152–167.

Shabani, A., Woznicki, S.A., Mehaffey, M., Butcher, J., Wool, T.A., Whung, P.Y., 2021. A coupled hydrodynamic (HEC-RAS 2D) and water quality model (WASP) for simulating flood-induced soil, sediment, and contaminant transport. J. Flood Risk Manag. 14 (4), e12747.

Sharif, H., Al-zahrani, M., Hassan, A.E., 2017. Driven by GPM satellite rainfall over an urbanizing arid catchment in Saudi Arabia.

Sharif, H.O., Chintalapudi, S., Hassan, A.A., Xie, H., Zeitler, J., 2013. Physically based hydrological modeling of the 2002 floods in San Antonio, Texas. J. Hydrol. Eng. 18 (2), 228–236.

Sharif, H.O., Sparks, L., Hassan, A.A., Zeitler, J., Xie, H., 2010. Application of a distributed hydrologic model to the November 17, 2004, flood of Bull Creek watershed, Austin, Texas. J. Hydrol. Eng. 15 (8), 651–657.

Shaw, S.B., Walter, M.T., Steenhuis, T.S., 2006. A physical model of particulate wash-off from rough impervious surfaces. J. Hydrol. 327 (3–4), 618–626.

Souza, C.M., Z. Shimbo, J., Rosa, M.R., Parente, L.L., A. Alencar, A., Rudorff, B.F.T., Hasenack, H., Matsumoto, M., G. Ferreira, L., Souza-Filho, P.W.M., de Oliveira, S.W., Rocha, W.F., Fonseca, A.V., Marques, C.B., Diniz, C.G., Costa, D., Monteiro, D., Rosa, E.R., Vélez-Martin, E., Weber, E.J., Lenti, F.E.B., Paternost, F.F., Pareyn, F.G.C., Siqueira, J.V., Viera, J.L., Neto, L.C.F., Saraiva, M.M., Sales, M.H., Salgado, M.P.G., Vasconcelos, R., Galano, S., Mesquita, V.V., Azevedo, T., 2020. Reconstructing three decades of land use and land cover changes in Brazilian biomes with landsat archive and earth engine. Remote Sens. 12 (17), http://dx.doi.org/10.3390/rs12172735, URL https://www.mdpi.com/2072-4292/12/17/2735.

Tu, M.C., Smith, P., 2018. Modeling pollutant buildup and washoff parameters for SWMM based on land use in a semiarid urban watershed. Water Air Soil Pollut. 229 (4), 1–15.

Vartziotis, E., Ulm, F., Boukin, K., Pellenq, R.J., Magnin, Y., Ioannidou, K., 2022. Modeling inundation flooding in urban environments using density functional theory.

Vieira, J.D., 1983. Conditions governing the use of approximations for the Saint-Venant equations for shallow surface water flow. J. Hydrol. 60 (1–4), 43–58.

Volk, M., Bosch, D., Nangia, V., Narasimhan, B., 2016. SWAT: Agricultural water and nonpoint source pollution management at a watershed scale. Agricult. Water Manag. 175, 1–3.

Wicke, D., Cochrane, T., O'sullivan, A., 2012. Build-up dynamics of heavy metals deposited on impermeable urban surfaces. J. Environ. Manag. 113, 347–354.

Wijesiri, B., Egodawatta, P., McGree, J., Goonetilleke, A., 2015a. Influence of pollutant build-up on variability in wash-off from urban road surfaces. Sci. Total Environ. 527, 344–350.

Wijesiri, B., Egodawatta, P., McGree, J., Goonetilleke, A., 2015b. Process variability of pollutant build-up on urban road surfaces. Sci. Total Environ. 518, 434–440.

Xiao, Y., Zhang, T., Wang, L., Liang, D., Xu, X., 2017. Analytical and experimental study on dissolved pollutant wash-off over impervious surfaces. Hydrol. Process. 31 (25), 4520–4529.

Yanxia, S., Qi, Z., Chunbo, J., 2022. A dynamic bidirectional coupling model for watershed water environment simulation based on the multi-grid technique. Sci. Total Environ. 843, 156760.

Zaffani, A.G., Mendiondo, E.M., 2012. Poluição difusa da drenagem urbana com base ecohidrológica: diagnóstico atual e cenários de longo prazo em bacias urbanas de são carlos, sp.

Zhang, K., Deletic, A., Bach, P.M., Shi, B., Hathaway, J.M., McCarthy, D.T., 2019. Testing of new stormwater pollution build-up algorithms informed by a genetic programming approach. J. Environ. Manag. 241, 12–21.

Zhang, T., Xiao, Y., Liang, D., Tang, H., Xu, J., Yuan, S., Luan, B., 2020. A physically-based model for dissolved pollutant transport over impervious surfaces. J. Hydrol. 590, 125478.

Zia, H., Harris, N.R., Merrett, G.V., Rivers, M., Coles, N., 2013. The impact of agricultural activities on water quality: A case for collaborative catchment-scale management using integrated wireless sensor networks. Comput. Electron. Agric. 96, 126–138.